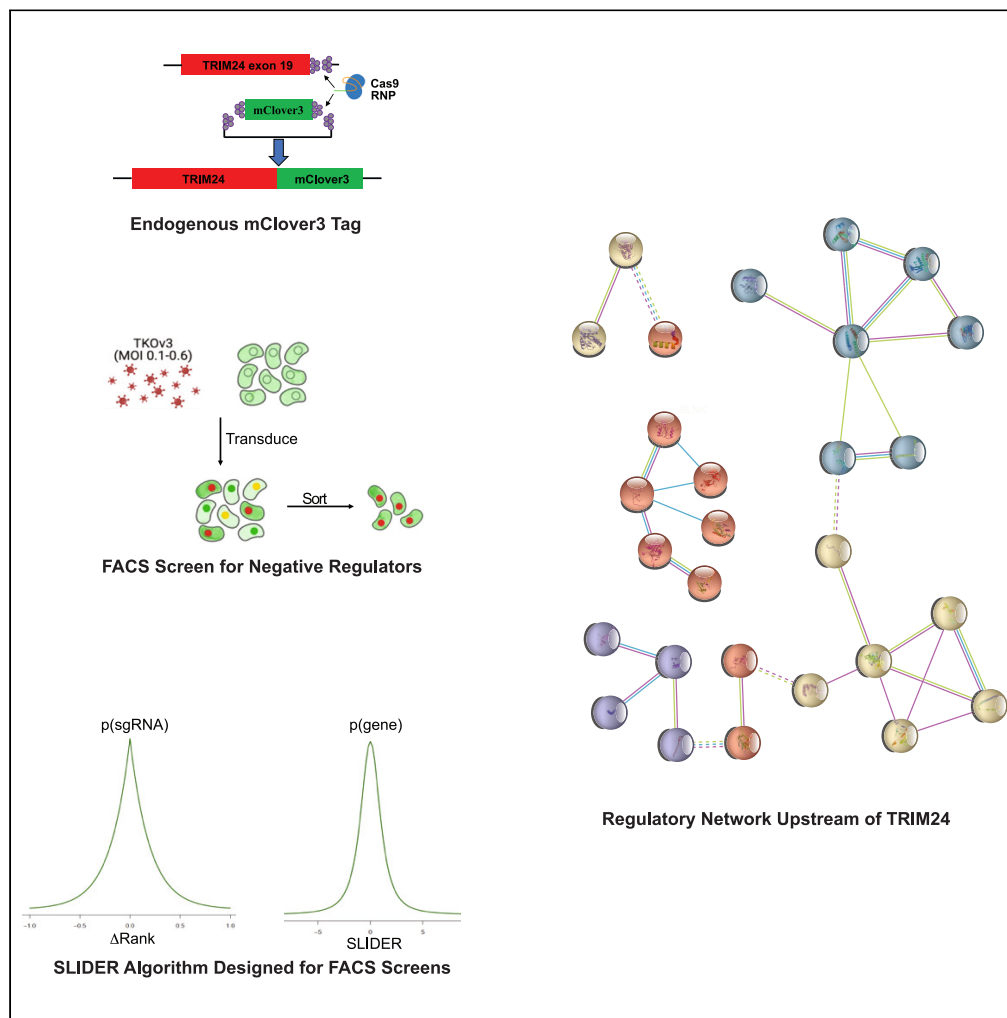


Article

Genome-wide CRISPR-Cas9 screen analyzed by SLIDER identifies network of repressor complexes that regulate TRIM24



Lalit R. Patel,
Sabrina A.
Stratton, Megan
McLaughlin, ...,
Daniela Barbosa,
Traver Hart,
Michelle C. Barton

lalit.patel@emory.edu (L.R.P.)
bartonsh@ohsu.edu (M.C.B.)

Highlights

In-frame *mClover3*
knockin enables FACS
screens of endogenous
TRIM24 regulation

SLIDER is designed for
analysis of FACS screens
and outperforms other
algorithms

TRIM28 negatively
regulates *TRIM24*
expression

Kap1, CNOT, and GID/
CTLH form network of
repressor complexes that
regulate *TRIM24*



Article

Genome-wide CRISPR-Cas9 screen analyzed by SLIDER identifies network of repressor complexes that regulate TRIM24

Lalit R. Patel,^{1,2,3,*} Sabrina A. Stratton,⁴ Megan McLaughlin,⁵ Patrick Krause,⁷ Kendra Allton,⁸ Andrés López Rivas,⁹ Daniela Barbosa,¹⁰ Traver Hart,^{5,6} and Michelle C. Barton^{11,12,*}

SUMMARY

TRIM24 is an oncogenic chromatin reader that is frequently overexpressed in human tumors and associated with poor prognosis. However, TRIM24 is rarely mutated, duplicated, or rearranged in cancer. This raises questions about how TRIM24 is regulated and what changes in its regulation are responsible for its overexpression. Here, we perform a genome-wide CRISPR-Cas9 screen by fluorescence-activated cell sorting (FACS) that nominated 220 negative regulators and elucidated a regulatory network that includes the KAP1 corepressor, CNOT deadenylase, and GID/CTLH E3 ligase. Knocking out required components of these three complexes caused TRIM24 overexpression, confirming their negative regulation of TRIM24. Our findings identify regulators of TRIM24 that nominate previously unexplored contexts for this oncoprotein in biology and disease. These findings were enabled by SLIDER, a new scoring system designed and vetted in our study as a broadly applicable tool for analysis of CRISPR screens performed by FACS.

INTRODUCTION

Oncogene activation is a formative event in carcinogenesis that leads to unregulated proliferation by tumor cells. Activation occurs when proto-oncogenes escape regulation because of mutations and rearrangements creating constitutively active variants or by changes in the cancer genome that rewire regulatory networks upstream of proto-oncogenes. This includes *cis*-acting genetic events that occur at the locus of a proto-oncogene and *trans*-acting events like deletion of negative regulators or duplication of an upstream activator.

TRIM24 is a causal oncogene that transforms human mammary epithelial cells when overexpressed *in vitro*,¹ causes spontaneous mammary tumorigenesis in genetically engineered mouse models *in vivo*,² promotes prostate adenocarcinoma formation as a ligand independent androgen receptor coactivator,³ and contributes to chemotherapy-resistant proliferation in glioblastoma by transcriptionally activating *PIK3CA* and *MGMT*.⁴ Immunohistochemical (IHC) analysis of several independent human tumor cohorts have also shown that TRIM24 is frequently overexpressed and associated with poor outcome across anatomic sites.^{3–14} Despite growing evidence for TRIM24's oncogenic function, little is known about how it is regulated and why it is aberrantly overexpressed in multiple cancers.

TRIM24 is rarely mutated or focally amplified in human tumors profiled by The Cancer Genome Atlas (TCGA),¹⁵ making it ripe for assessment of a rewired regulatory network. Molecular studies show TRIM24 is recruited by SPOP (Speckle Type BTB/POZ Protein) for ubiquitination,¹⁶ auto-ubiquitinated when phosphorylated by ATM (Ataxia-telangiectasia mutated),¹⁷ and protected from the proteasome when heterodimerized to other tripartite motif proteins.¹⁸ Although these findings suggest a role for post-translational control, no global systematic probe of TRIM24 regulation has been undertaken, leaving its larger regulatory network unknown.

We address this by performing a genome-wide CRISPR/Cas9 screen for negative regulators of TRIM24 that is enabled by two innovations. We engineered cell lines by integrating the coding sequence of a fluorescent-protein into the endogenous TRIM24 gene to enable a screen that captures regulation by epigenetic,

¹Department of Genetics, University of Texas MD Anderson Cancer Center, Houston, TX, USA

²University of Texas MD Anderson Cancer Center UTHHealth Graduate School of Biomedical Sciences, University of Texas, Houston, TX, USA

³McGovern Medical School, University of Texas Health Science Center at Houston, Houston, TX, USA

⁴Department of Epigenetics and Molecular Carcinogenesis, The University of Texas MD Anderson Cancer Center, Houston, TX, USA

⁵Department of Bioinformatics and Computational Biology, The University of Texas MD Anderson Cancer Center, Houston, TX, USA

⁶Department of Cancer Biology, The University of Texas MD Anderson Cancer Center, Houston, TX, USA

⁷Department of Cancer Biology, University of Cincinnati College of Medicine, Cincinnati, OH, USA

⁸The Neurodegeneration Consortium, Therapeutics Discovery, University of Texas MD Anderson Cancer Center, Houston, TX, USA

⁹School of Medicine, University of Puerto Rico Medical Sciences Campus, San Juan, PR, USA

¹⁰Department of Molecular Biology, University of Texas Southwestern, Dallas, TX, USA

¹¹Division of Oncological Sciences, Cancer Early Detection Advanced Research Center, Knight Cancer Institute, Oregon Health & Science University, Portland, OR, US

Continued



transcriptional, and post-translational effectors. We also created a scoring algorithm designed specifically for data from screens that compare cells collected by fluorescence-activated cell sorting (FACS) to cells from an unsorted control. Candidates from our screen identify a network of protein complexes and cellular processes that downregulate *TRIM24*, providing the first systems-biology insight into how *TRIM24* is regulated. In this study, we validate three protein complexes from the elucidated network and present a screening and analysis platform that is generalizable to targets at large.

RESULTS

Engineering cell lines with an endogenous fluorescent protein tag on *TRIM24*

Screening for regulators of *TRIM24* requires a platform in which the effects of genetic perturbation on *TRIM24* expression are readily observed and cells with different levels of expression can be collected. Fluorescence-activated cell sorting (FACS) of cells expressing fluorescently tagged protein provides an ideal solution. Typically, this is accomplished using ectopic constructs. However, ectopic constructs suffer from a number of limitations. They do not preserve the gene's chromatin environment or retain its 5'UTR. Ectopic expression is also driven by a constitutive promoter which leads to super-physiologic expression. Screens using these constructs therefore likely miss regulation by epigenetic, transcriptional, and physiologic processes while favoring nomination of regulators that are more active when a gene is already overexpressed.

To overcome these limitations, we genetically engineered cell lines with an in-frame knock-in of *mClover3*, a brighter monomeric mutant of *GFP* (green fluorescent protein),¹⁹ to *TRIM24* proximal and upstream of the stop codon (Figure 1A, STAR Methods). The edit renders *TRIM24*, expressed physiologically from a cell's native copy, fluorescent and achieves tagging without sacrificing endogenous regulation. To capture regulation in cellular lineages where *TRIM24* has demonstrated oncogenic function,^{2–4} the knock-in was performed in spontaneously immortalized MCF10A breast epithelial cells, HPV immortalized RWPE prostate epithelial cells (also known as RWPE1 cells), and U251 glioblastoma cells. To select for cells with on-target knock-in without off-target integration, we isolated clones and selectively expanded those that have a single copy of *mClover3* and a single copy of the expected junction between exon19 of *TRIM24* and *mClover3* as assessed by ddPCR. This yielded two clones per cell line with mono-allelic on-target singular integration of *mClover3* (Figure 1B). MCF10A clones were named C6 and C9, RWPE clones were named R3 and R7, and U251 clones were named U7 and U8. Spanning PCR amplicons are consistent with ddPCR findings showing that MCF10A and U251 clones have heterozygous knock-in with preservation of their untagged alleles while RWPE clones have knock-in with loss of the untagged copy (Figure 1C). Sanger sequencing of knock-in amplicons confirmed in-frame integration (Figure S1). Knock-in clonal lines also show the expected bands for wild-type and *mClover3*-tagged *TRIM24* protein by western blot (Figure 1D) and have increased GFP fluorescence by flow cytometry when compared to unedited parental cells (Figures 1E, 1F, and S2A). Targeted CRISPR-knockout of *TRIM24* abolished this fluorescence (Figures 1G, 1H, and S2A). A reciprocal experiment using dCas9-VP64 for CRISPR-activation of *TRIM24* increased GFP signal (Figures 1I, 1J, and S2B). Together these experiments show GFP signal in our clones is specific to *TRIM24* and responsive to increased *TRIM24* expression.

Additional concerns stemming from the use of a fluorescent protein tag include mislocalization, allelic preference, and changes in protein stability. To assess these concerns, we assessed *TRIM24* protein localization and stability in MCF10A clones, which express both endogenously tagged and unedited *TRIM24* (Figures 1C and 1D). Cell fractionation showed no change between tagged and unedited *TRIM24*'s distribution between cytoplasmic, soluble nuclear, or chromatin bound fractions (Figure S2C). This confirmed that the carboxy-terminal (C-terminal) tag engineered by our knock-in did not interfere with *TRIM24*'s chromatin binding, a function attributed to its C-terminal histone reader PHD/bromodomains.¹³ Passaging edited clones did not lead to either tagged or unedited *TRIM24* becoming predominantly expressed (Figures S2D and S2E), suggesting no allelic preference. No significant difference was observed in *TRIM24* protein stability assayed in cycloheximide chase experiments comparing untagged to tagged *TRIM24* (Figures S2F and S2G). These biochemical controls lend confidence to the claim that the fluorescent *TRIM24*-*mClover3* protein expressed from the endogenously tagged copy of *TRIM24* remains subject to the same regulatory controls as *TRIM24* protein expressed from an unedited allele.

Before screening a genome-wide library by FACS for regulators of *TRIM24*, we performed two proof-of-principle screens of small sgRNA pools to assess whether FACS of our knock-in tagged cells lines can enrich

¹²Lead contact

*Correspondence:

lalit.patel@emory.edu

(L.R.P.),

bartonsh@ohsu.edu (M.C.B.)

<https://doi.org/10.1016/j.isci.2023.107126>

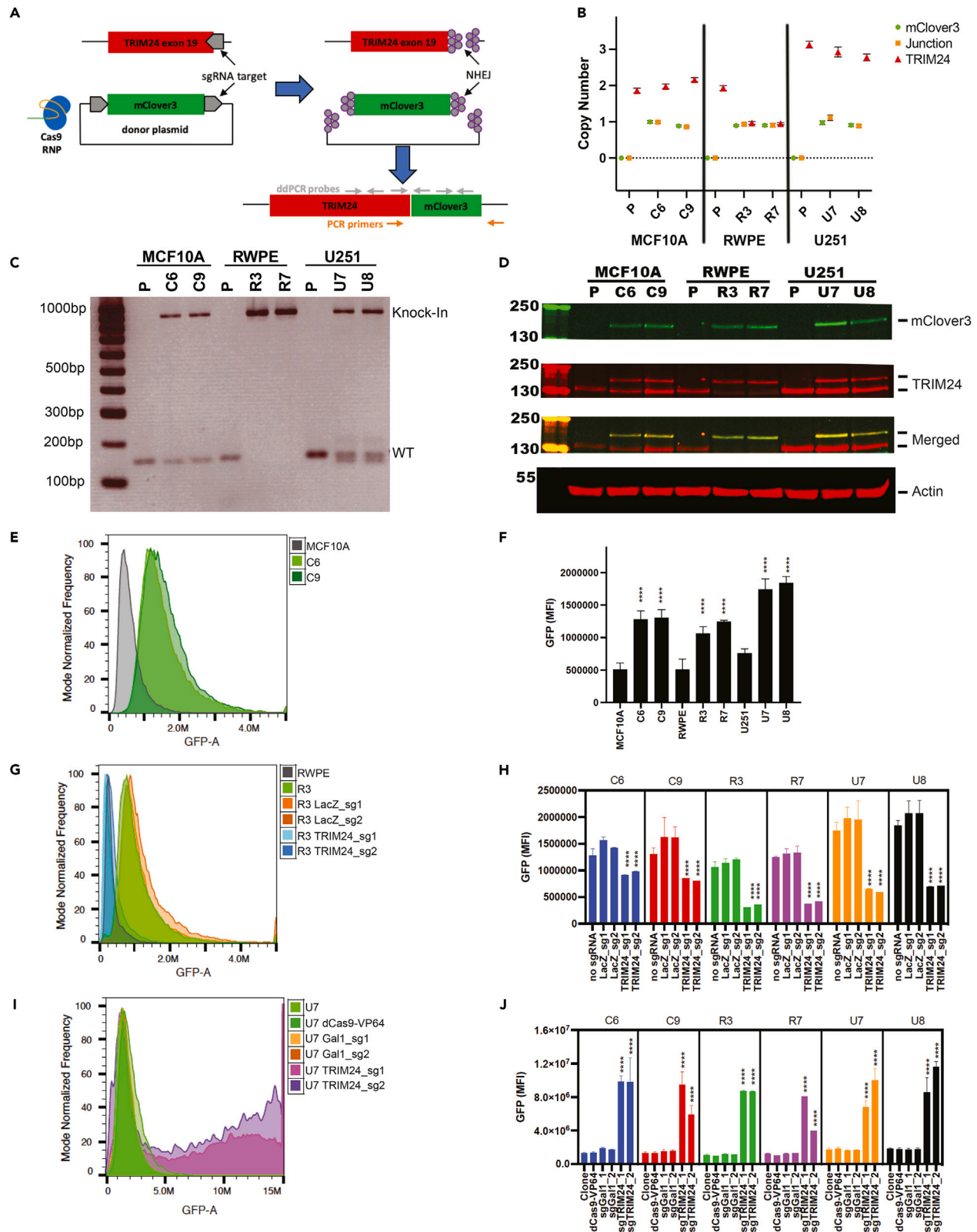


Figure 1. Engineering and validation of cell lines with an endogenous fluorescent protein tag to TRIM24

- (A) Schematic of Homology Independent Target Integration (HITI) using a recombinant Cas9-RNP and donor plasmid to perform in-frame knock-in of mClover3 to exon19 of TRIM24.
- (B) Copy number determined using ddPCR of mClover3, TRIM24, and the junction expected between the two in a successful knock-in. Assay performed in two successful knock-in clones per cell line with unedited parental cells (P) as controls and copy number of the RPP30 as an internal control.
- (C) Spanning PCR amplicons from parental and edited clones demonstrate an expected knock-in product that is ~720bp longer in edited clones than the ~150bp amplicon expected for unedited TRIM24.
- (D) Western blot demonstrating expression of endogenously tagged TRIM24 protein in edited clones. mClover3-tagged protein is resolved as a higher molecular weight band when probed with antibody to TRIM24 that is also positive for mClover3 when probed with an antibody to GFP.
- (E) Histogram of GFP-channel fluorescence (GFP-A) assayed by flow cytometry comparing knock-in clones to parental MCF10A control cells (for all lines see [Figure S1A](#)).
- (F) Average GFP channel mean fluorescence intensity (GFP MFI) of edited clones and their respective unedited parental cell line control. Increase in GFP MFI of edited clones compared to parental cell controls is statistically significant.
- (G) GFP-A histogram of endogenously tagged clone R3 transduced with sgRNA knocking out TRIM24 or negative controls targeting LacZ. Parental RWPE cells are shown as an auto-fluorescence control (for all lines see [Figure S1A](#)).
- (H) Average GFP MFI of untransduced clones and clones transduced with sgRNA targeting TRIM24 for knockout or LacZ targeting negative controls. GFP signal is significantly reduced in all 6 clones by either TRIM24 targeting sgRNA when compared to untransduced controls.
- (I) GFP-A Histogram of endogenously tagged clone U7 without transduction, transduced with dCas9-VP64 alone, or transduced with dCas9-VP64 and activating guides targeting the promoter of TRIM24 or the promoter of yeast Gal1 as a negative control (for all lines see [Figure S1B](#)).
- (J) Average GFP MFI in clones without transduction, transduced with dCas9-VP64 alone, or transduced with dCas9-VP64 and activating guides targeting the promoter of TRIM24 or the promoter of yeast Gal1 as a negative control. GFP signal was significantly increased in clones with TRIM24 activating sgRNA compared to clones transduced with dCas9-VP64 alone as a control. F,H,J) Comparisons made using Student's t test, **** represents $p < 1e-3$.

for sgRNA expected to increase TRIM24 protein in cells. The first screened an equimolar pool of three sgRNA targeting *SPOP*, a known negative regulator of *TRIM24*,^{3,16,18} for knockout by Cas9 and three sgRNA targeting *LacZ* as negative controls. The second used dCas9-VP64 to activate genes and an equimolar pool of three *TRIM24* promoter targeting sgRNA and three guides activating the yeast gene *Gal1* as negative controls. The expectation is that *SPOP* targeting sgRNA would be enriched from our knockout pool, *TRIM24* activating guides would be enriched from our activating pool, and negative control guides would be depleted from both pools after sorting for cells with high GFP. Both experiments produced the expected results ([Figures S2H](#) and [S2I](#)), supporting the use of endogenously tagged cell lines in FACS screens for regulators.

SLIDER: A scoring system for screens using cell sorting

Functional genomic screens performed by cell sorting differ from proliferation screens ([Figure 2A](#)). Proliferation screens rely on population dynamics to enrich or deplete perturbations that change cellular fitness under biological conditions chosen by an investigator. When a defined subset of genes is responsible for context-specific fitness, most reagents in a diverse library will have no effect. This allows sgRNAs that are normally distributed at the outset of a screen to maintain a normal distribution at the end, with an expected value of zero for changes in read count between the beginning and end of a screen. These conditions allow changes in read count to serve as a statistically scorable metric for sgRNA activity in proliferation screens. In contrast, sorting depletes the majority of a population, causes a minority of perturbations to dominate read counts, and results in post-screen populations that are skewed or exponential depending on how stringently a sort is performed. Guides that have no effect on the signal being sorted for therefore experience large changes in read count, making methods that rely on changes in counts a poor fit for analysis of FACS screens.

To address this, we devised a scoring system that utilizes changes in rank before and after sorting as its underlying basis. We call this algorithm SLIDER for scoring sorting screens using Laplace and differential ranks ([Figure 2B](#), [STAR Methods](#), [Data S1](#)). The algorithm makes three assumptions.

- (1) Changes in sgRNA rank caused by sorting when normalized by the size of the library follow a biexponential Laplace distribution with an expected value of zero
- (2) The diversity of change in rank is a function of the sgRNA's unsorted rank and the direction (increase or decrease) in which rank is changed
- (3) SLIDER scores computed using the weighted logit method are well represented by a Student's t-distribution with 2° of freedom

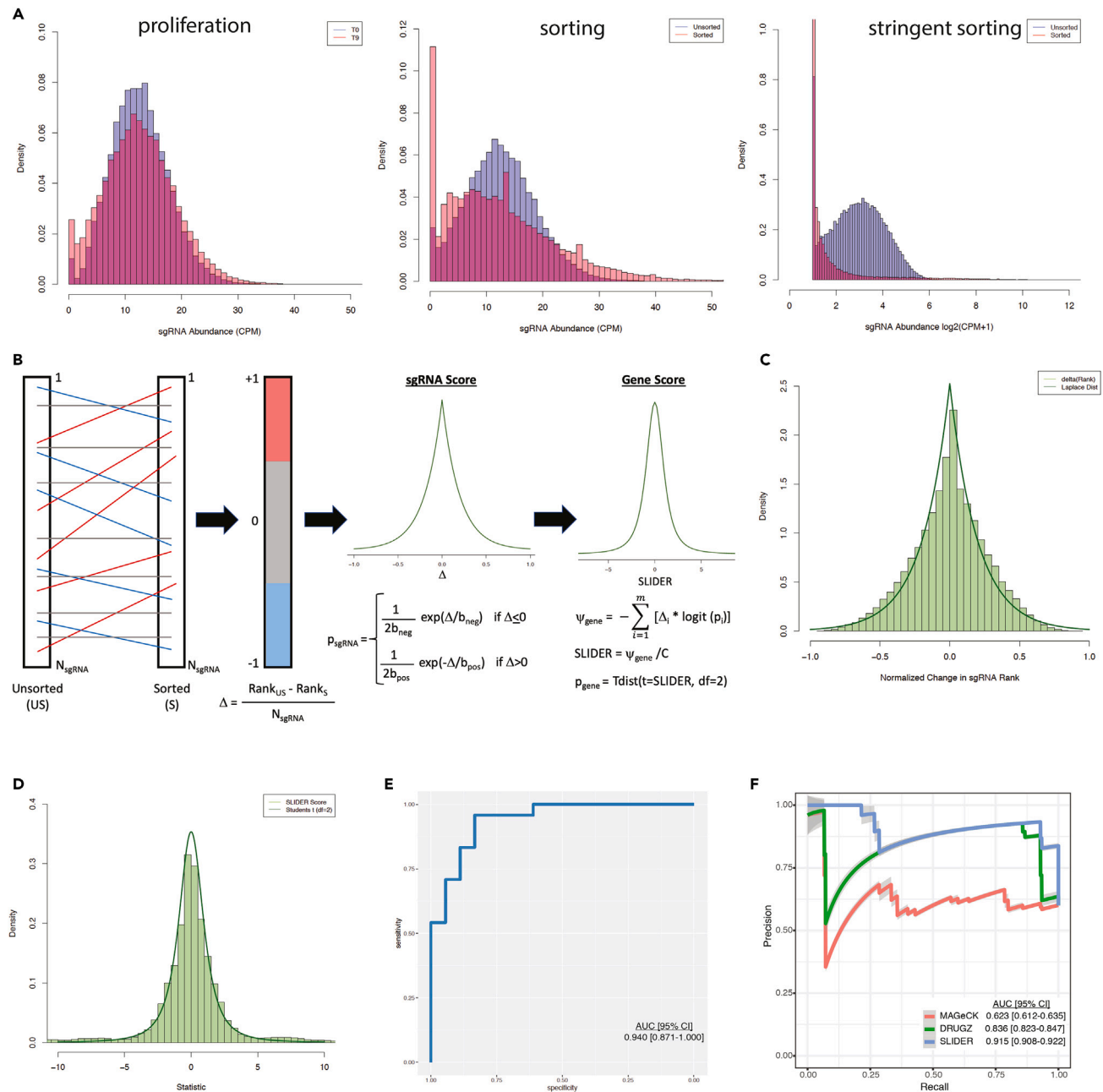


Figure 2. SLIDER – A scoring system designed for sorting screens that outperforms popular counts based methods

(A) Representative pre- and post-selection histograms from published screens that illustrate the different effects of proliferation and sorting on sgRNA read counts. Proliferation histogram shows the effect of passaging cells transduced with a genome-wide library for 9 days and Sorting histogram shows the effect of FACS with a 2% gate in a screen for genes acting on a splicing reporter, both from GSE112599 (Gonatopoulos-Pournatzis et al., 2018). Stringent Sorting histogram shows the effect of serial sorting to obtain a purified GFP+ population in a screen for endoplasmic reticulum associated degradation effectors (Timms et al., 2016). Stringent Sorting histogram presented with log-scaled counts to include the larger range of sgRNA counts spanned by this dataset.

(B) Schematic diagram depicting the SLIDER algorithm.

(C) Laplace distribution over histogram of normalized change in rank (Δ) from a representative replicate of a sorting screen.

(D) Student's t-distribution with 2° of freedom over histogram of SLIDER scores calculated using the same replicate as panel C.

(E) Receiver Operator Characterization assessing performance of SLIDER as a scoring system identifying 24 positive regulators of a splicing-reporter from a list of 42 genes containing 18 expected negatives using data from a published and validated splicing-reporter screen. C-E) Data from a published FACS sorted Mef2d-splicing-reporter screen (Gonatopoulos-Pournatzis et al., 2018).

(F) Precision Recall Analysis comparing performance of MAGeK, DrugZ, and SLIDER scores determined from NGS readouts of our screen as predictors of validation experiments presented in this study (see Figure 3).

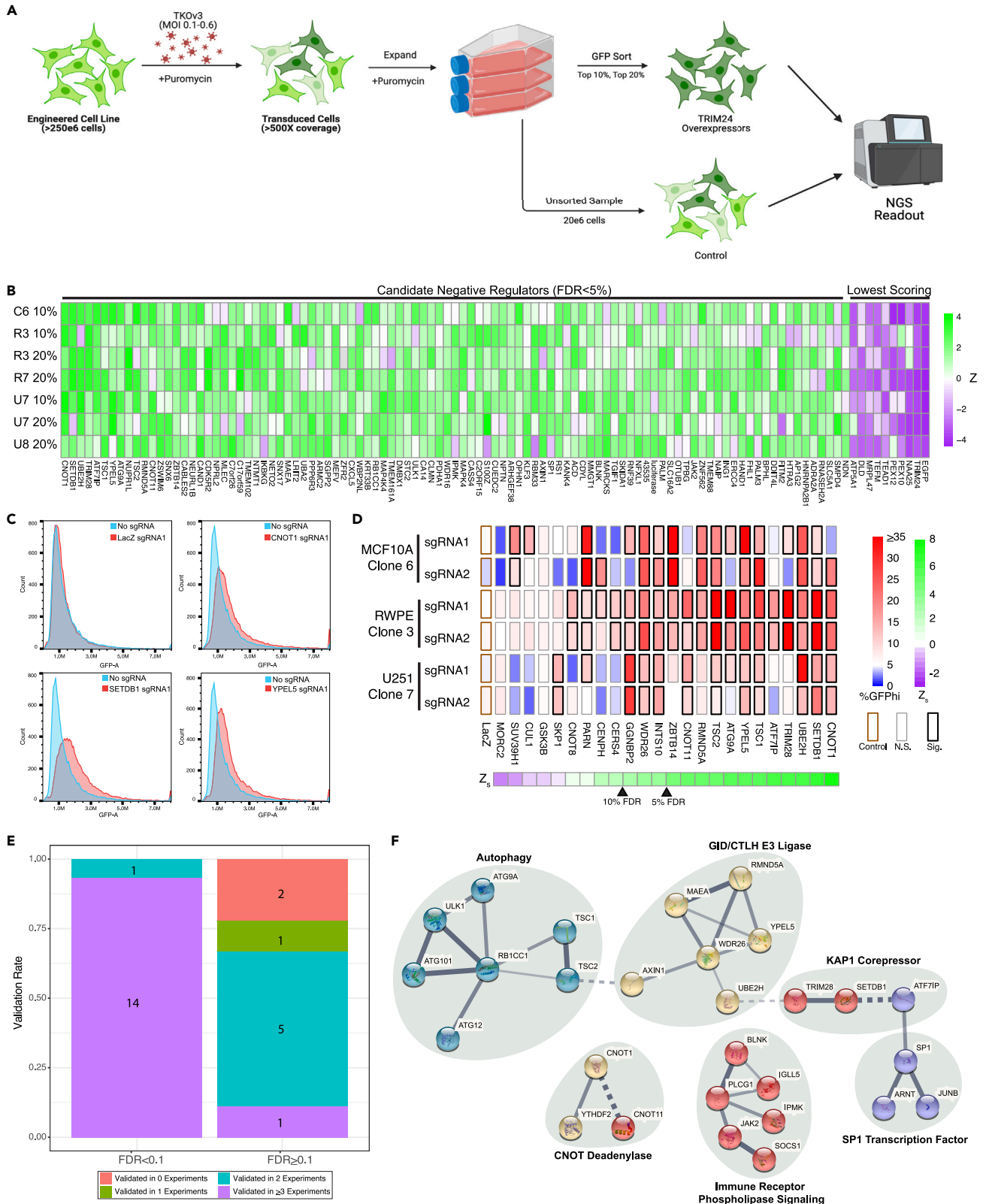


Figure 3. Genome-wide CRISPR/Cas9 screen for negative regulators of TRIM24 identifies a network of protein complexes and cellular processes

(A) Schematic diagram of Fluorescence-Activated Cell Sorting (FACS) screen performed using the TKOv3 CRISPR-knockout library and cell lines engineered with endogenous mClover3 tagged TRIM24.

(B) Heatmap of Z-scores from SLIDER for the 99 genes nominated with an FDR<5% and the 10 lowest scoring genes. TRIM24 and EGFP serve as internal controls for adequate sorting and Cas9 activity by showing the expected outcome of becoming the two most depleted genes in the screen.

(C) Representative histograms of GFP channel fluorescence (GFP-A) obtained in validation experiments summarized in panel D.

(D) Validation experiments performed using one mClover3 tagged clone per cell line and 2 sgRNA per gene for 24 genes spanning a wide range of scores from SLIDER. sgRNA targeting LacZ are included as negative controls. GFP^{hi} cells were defined for each clone by gating for 5% of live single cells with the highest GFP-A in a randomly selected replicate of the clone transduced with LacZ sgRNA1. A significant increase in %GFP^{hi} cells was determined using a one-sided Z-test against LacZ controls with Bonferroni correction for multiple testing and $\alpha = 0.05$.

(E) Fraction of genes in the validation study that validated when categorized by meeting an FDR threshold of 10%. Genes are considered true negative regulators if they validate in at least 3 independent assays of the 6-fold (3 lines x 2 sgRNA) validation study described.

(F) Negative regulatory network identified from the 150 highest scoring genes in our screen (FDR<7.1%) using STRING and filtering for subnetworks with at least 3-nodes.

Analysis of four published FACS screens from three studies with publicly deposited data^{20–22} found each to be concordant with these assumptions, despite using different cell lines, reporters, and libraries (Figures 2C, 2D, and S3A). SLIDER's diverse utility for analysis of various sorting screens is also demonstrated by reanalysis of published screens (Figures S3B–S3D). This includes rediscovery of three CRISPRa Response Elements (CaREs) upstream of the CD69 gene,²² rediscovery of 17 of 22 regulators of endoplasmic reticulum associated degradation in a single stringently sorted replicate from a study that initially discovered them using two separate screening platforms,²³ and finding 126 candidate negative regulators for the gene *Srrm4* at an FDR<1% when the published study nominated zero with FDR <10%.²⁰

Performance was further evaluated by ROC analysis, which yielded an AUC of 0.94 (Figure 2E) for gene scores from SLIDER as predictors of the results of a splicing reporter screen with extensive validation.²⁰ Because candidates for validation in that study were selected using MAGeCK, a performance comparison was not possible using their data. Using our own screen and validation assays (Figures 3B and 3D), SLIDER outperformed two counts-based methods, MAGeCK and DrugZ, in a precision recall analysis with an AUC of 0.915 (Figure 2F).

Genome-wide CRISPR-Cas9 screen identifies negative regulators of TRIM24

The six knock-in clonal cell lines engineered to express endogenously tagged TRIM24-mClover3 (Figure 1) were transduced with the TKOv3 genome-wide CRISPR-Cas9 knockout library containing 70948 sgRNA targeting 18053 genes in addition to 142 control guides targeting *EGFP*, *LacZ*, and *Luciferase* (Figure 3A). Transduced cells were expanded and sorted for GFP-hi cells using a 10% (clonal lines C6, R3, U7) or a 20% (all six clonal lines) sorting gate for a total of nine biologically independent screen replicates. At each sort, an unsorted sample was taken as a paired control. Cell counts were monitored throughout the transduction, expansion, and sorting process to assure adequate sampling and coverage of the library (see STAR Methods, Figures 3A and S4A). Two of the replicates, clones C6 and C9 with a 20% gate, had poor next-generation sequencing readouts and were excluded from further analysis (Figures S4B and S4C). The remaining seven replicates were analyzed using SLIDER, which identified 99 candidate negative regulators with a false discovery rate (FDR) < 5% and 220 candidates with FDR <10%. The two genes most depleted by sorting across analyzed replicates were EGFP and TRIM24, an expected result confirming active cutting by Cas9 and adequate sorting in our screen (Figure 3B, Data S3).

To validate our screen, we selected 24 genes spanning a broad range of scores. This included 12 genes with an FDR<5%, 12 genes with an FDR>5%, and nine with an FDR>10% to evaluate false-positive and false-negative rates (Figure 3D). We then assessed by flow cytometry (Figures 3C and S5A) whether TRIM24-mClover3 expression increased as predicted by our screen when these genes were knocked out using two independent sgRNA per gene and two sgRNA against LacZ as negative controls (Table 1). The experiment was performed in three of our endogenously tagged lines, providing 6 independent experiments per gene (Figure 3D). Increases were considered biologically true if they were statistically significant in $\geq 3/6$ experiments. At an FDR of 10%, 14/15 nominated genes validated, 1/15 candidates did not, and one gene with FDR>10% validated (Figures 3E and S5B and S5C). This corresponds to an overall performance of 88.9% sensitivity and 93.3% specificity for candidates nominated at this threshold (Figure S5D). Given the high quality this suggests for hits from our screen, we performed a network analysis in STRING using the 150 highest scoring genes (FDR<7.1%). STRING identified a network of 6 gene clusters containing ≥ 3 nodes

Table 1. Summary of flow cytometry experiments Associated with single gene perturbation studies, related to Figure 3D

Cell Line	Gene sgRNA	SLIDER Z	Replicates by Flow Cytometry, %GFP OE gated at 5% using LacZ sgRNA1											
			Sample 1	Sample 2	Sample 3	Sample 4	Sample 5	Sample 6	Sample 7	Sample 8	Sample 9	Sample 10	Sample 11	Sample 12
MCF10A C6	LacZ sgRNA1	-0.2443	5.04	4.82	4.72	5.13	6.44	5.99	5.89	6.36				
MCF10A C6	LacZ sgRNA2	-0.2443	5.11	5.12	5.13	5.01	2.59	3.13	3.19	2.56				
MCF10A C6	MORC2 sgRNA1	-1.3205	1.78	1.67	1.67	1.59								
MCF10A C6	MORC2 sgRNA2	-1.3205	1.15	1.48	1.16	1.25								
MCF10A C6	SUV39H1 sgRNA1	-1.1116	19.4	19.7	18.5	18.8								
MCF10A C6	SUV39H1 sgRNA2	-1.1116	8.58	8.67	8.7	8.41								
MCF10A C6	CUL1 sgRNA1	-0.3767	14.7	14.1	14.5	13.3								
MCF10A C6	CUL1 sgRNA2	-0.3767	6.17	5.89	5.83	6.12								
MCF10A C6	GSK3B sgRNA1	-0.2266	6.7	6.7	6.88	7.73								
MCF10A C6	GSK3B sgRNA2	-0.2266	6.79	7.36	6.7	6.78								
MCF10A C6	SKP1 sgRNA1	-0.0153	5.02	5	4.7	5.41								
MCF10A C6	SKP1 sgRNA2	-0.0153	2.18	2.44	2.2	2.41								
MCF10A C6	CNOT8 sgRNA1	1.0027	6.53	7.64	6.67	6.41								
MCF10A C6	CNOT8 sgRNA2	1.0027	1.95	1.71	1.58	1.78								
MCF10A C6	PARN sgRNA1	1.0393	33.2	32.5	31.7	30.5								
MCF10A C6	PARN sgRNA2	1.0393	52.1	49.9	46	53.6								
MCF10A C6	CENPH sgRNA1	2.1881	2.56	2.42	2.2	2.3								
MCF10A C6	CENPH sgRNA2	2.1881	18	19.2	19.1	17.3								
MCF10A C6	CERS4 sgRNA1	2.4173	2.29	2.08	2.17	1.85								
MCF10A C6	CERS4 sgRNA2	2.4173	4.07	3.75	3.81	3.59								
MCF10A C6	GGNBP2 sgRNA1	3.0529	13.3	13.6	13	15.9								
MCF10A C6	GGNBP2 sgRNA2	3.0529	2.9	2.63	2.62	2.55								
MCF10A C6	WDR26 sgRNA1	3.2627	24.8	23.8	22.9	21.9								
MCF10A C6	WDR26 sgRNA2	3.2627	26.4	24.2	22.5	27.7								
MCF10A C6	INTS10 sgRNA1	3.2976	10.9	12.1	11.5	11.4								
MCF10A C6	INTS10 sgRNA2	3.2976	18.7	17.4	17.6	18.7								
MCF10A C6	ZBTB14 sgRNA1	4.7700	58.6	59.1	58.9	60.3								
MCF10A C6	ZBTB14 sgRNA2	4.7700	36.6	36.9	37.2	37.3								
MCF10A C6	CNOT11 sgRNA1	4.8411	4.23	3.22	4.21	4.4								
MCF10A C6	CNOT11 sgRNA2	4.8411	6.29	6.68	6.42	5.83								
MCF10A C6	RMND5A sgRNA1	4.8568	20.6	19	16.3	21.3								
MCF10A C6	RMND5A sgRNA2	4.8568	23.5	24.2	23.8	23.8								
MCF10A C6	TSC2 sgRNA1	5.1805	9.9	20.9	21.4	22.9								

(Continued on next page)

Table 1. Continued

Cell Line	Gene sgRNA	SLIDER Z	Replicates by Flow Cytometry, %GFP OE gated at 5% using LacZ sgRNA1											
			Sample 1	Sample 2	Sample 3	Sample 4	Sample 5	Sample 6	Sample 7	Sample 8	Sample 9	Sample 10	Sample 11	Sample 12
MCF10A C6	TSC2 sgRNA2	5.1805	19.8	19.4	19.5	20.5								
MCF10A C6	ATG9A sgRNA1	5.3687	12.8	13.3	12.8	13.3								
MCF10A C6	ATG9A sgRNA2	5.3687	3.63	3.29	2.97	4.14								
MCF10A C6	YPEL5 sgRNA1	5.4951	37.4	36.9	36.6	35.7								
MCF10A C6	YPEL5 sgRNA2	5.4951	18	18.1	18.7	18.2								
MCF10A C6	TSC1 sgRNA1	5.5131	15.2	14.5	12.9	16.7								
MCF10A C6	TSC1 sgRNA2	5.5131	30.2	30.5	31.1	31.8								
MCF10A C6	ATF7IP sgRNA1	6.2464	5.46	5.27	4.2	3.74								
MCF10A C6	ATF7IP sgRNA2	6.2464	6.18	5.49	6.09	5.9								
MCF10A C6	TRIM28 sgRNA1	6.2484	9.01	9.1	8.61									
MCF10A C6	TRIM28 sgRNA2	6.2484	2.82	2.83	2.99	2.71								
MCF10A C6	UBE2H sgRNA1	6.3129	24.6	24.8	24.9	24.5								
MCF10A C6	UBE2H sgRNA2	6.3129	25.2	25.4	25.3	24.7								
MCF10A C6	SETDB1 sgRNA1	6.4616	9.92	8.95	8.78	10.2								
MCF10A C6	SETDB1 sgRNA2	6.4616	10.4	10.4	10.8	10.7								
MCF10A C6	CNOT1 sgRNA1	7.8476	3.35	3.45	3.13	3.44								
MCF10A C6	CNOT1 sgRNA2	7.8476	19.8	19.8	19.9	20.9								
RWPE R3	LacZ sgRNA1	-0.2443	4.92	4.96	4.53	4.48	5.49	5.74	5.63	5.98				
RWPE R3	LacZ sgRNA2	-0.2443	5.48	5.3	5.19	4.75	7.37	7.01	7.34	7.47				
RWPE R3	MORC2 sgRNA1	-1.3205	7.7	6.6	6.56	6.22								
RWPE R3	MORC2 sgRNA2	-1.3205	4.71	5.17	4.57	4.59								
RWPE R3	SUV39H1 sgRNA1	-1.1116	8.22	7.63	7.88	8								
RWPE R3	SUV39H1 sgRNA2	-1.1116	7.51	7.39	7.19	7.99								
RWPE R3	CUL1 sgRNA1	-0.3767	6.21	6.73	6.17	5.77								
RWPE R3	CUL1 sgRNA2	-0.3767	8.21	8.03	8.19	7.84								
RWPE R3	GSK3B sgRNA1	-0.2266	6.54	6.42	6.72	6.33								
RWPE R3	GSK3B sgRNA2	-0.2266	7.37	7.12	6.81	6.41								
RWPE R3	SKP1 sgRNA1	-0.0153	8.44	8.82	7.99	8.68								
RWPE R3	SKP1 sgRNA2	-0.0153	7.4	6.66	6.86	6.81								
RWPE R3	CNOT8 sgRNA1	1.0027	13.4	13	13.3	13.1								
RWPE R3	CNOT8 sgRNA2	1.0027	9.8	9.58	9.65	9.53								
RWPE R3	PARN sgRNA1	1.0393	9.8	9.56	9.41	9.26								
RWPE R3	PARN sgRNA2	1.0393	9.88	9.31	9.52	9.24								

(Continued on next page)

Table 1. Continued

Cell Line	Gene sgRNA	SLIDER Z	Replicates by Flow Cytometry, %GFP OE gated at 5% using LacZ sgRNA1											
			Sample 1	Sample 2	Sample 3	Sample 4	Sample 5	Sample 6	Sample 7	Sample 8	Sample 9	Sample 10	Sample 11	Sample 12
RWPE R3	CENPH sgRNA1	2.1881	10.5	10.2	10	10								
RWPE R3	CENPH sgRNA2	2.1881	8.17	8.56	8.95	7.95								
RWPE R3	CERS4 sgRNA1	2.4173	11.4	11.2	11.9	11.3								
RWPE R3	CERS4 sgRNA2	2.4173	12.2	11.3	10.6	10.9								
RWPE R3	GGNBP2 sgRNA1	3.0529	14.1	14	14.5	14								
RWPE R3	GGNBP2 sgRNA2	3.0529	11.9	11.5	11.5	11								
RWPE R3	WDR26 sgRNA1	3.2627	20.5	21.7	20.6	19.9								
RWPE R3	WDR26 sgRNA2	3.2627	26.2	26.5	26	25.2								
RWPE R3	INTS10 sgRNA1	3.2976	13.5	13.8	13.8	13.1								
RWPE R3	INTS10 sgRNA2	3.2976	16.5	16.4	16.3	16.2								
RWPE R3	ZBTB14 sgRNA1	4.7700	15.9	16.2	15.3	14.7								
RWPE R3	ZBTB14 sgRNA2	4.7700	14.3	12.9	13.1	12.4								
RWPE R3	CNOT11 sgRNA1	4.8411	23	22.9	22.3	24								
RWPE R3	CNOT11 sgRNA2	4.8411	10.7	10.1	11.2	10.1								
RWPE R3	RMND5A sgRNA1	4.8568	16.7	16.2	16.3	15.5								
RWPE R3	RMND5A sgRNA2	4.8568	16.3	16.1	16.1	15.8								
RWPE R3	TSC2 sgRNA1	5.1805	45.5	45.3	44.8	44.5								
RWPE R3	TSC2 sgRNA2	5.1805	39.5	38.8	38.6	38								
RWPE R3	ATG9A sgRNA1	5.3687	37.2	37.3	37.4	37.1								
RWPE R3	ATG9A sgRNA2	5.3687	17.8	18.4	17.6	17.6								
RWPE R3	YPEL5 sgRNA1	5.4951	20.8	20.8	20.1	19.3								
RWPE R3	YPEL5 sgRNA2	5.4951	24.8	24.4	24.4	24.5								
RWPE R3	TSC1 sgRNA1	5.5131	27.9	27.2	27.1	26.1								
RWPE R3	TSC1 sgRNA2	5.5131	19.4	19.9	20.3	19.4								
RWPE R3	ATF7IP sgRNA1	6.2464	17.9	17.5	17.5	17.5								
RWPE R3	ATF7IP sgRNA2	6.2464	14.2	14.3	13.9	13.9								
RWPE R3	TRIM28 sgRNA1	6.2484	58.9	59.7	59.5	60.3								
RWPE R3	TRIM28 sgRNA2	6.2484	39.1	38.8	38	37.3								
RWPE R3	UBE2H sgRNA1	6.3129	21.3	20.9	20.3	20.6								
RWPE R3	UBE2H sgRNA2	6.3129	16.8	17.1	16.5	16.3								
RWPE R3	SETDB1 sgRNA1	6.4616	43.4	42.8	42.6	42.5								
RWPE R3	SETDB1 sgRNA2	6.4616	35.5	35	35	35.1								
RWPE R3	CNOT1 sgRNA1	7.8476	23.6	23	22.4	22.6								

(Continued on next page)

Table 1. Continued

Cell Line	Gene sgRNA	SLIDER Z	Replicates by Flow Cytometry, %GFP OE gated at 5% using LacZ sgRNA1											
			Sample 1	Sample 2	Sample 3	Sample 4	Sample 5	Sample 6	Sample 7	Sample 8	Sample 9	Sample 10	Sample 11	Sample 12
RWPE R3	CNOT1 sgRNA2	7.8476	22.6	22.3	21.9	21.9								
U251 U7	LacZ sgRNA1	-0.2443	4.97	4.65	4.71	4.55	5.36	5.35	5.04	4.79	4.39	4.37	4.53	4.22
U251 U7	LacZ sgRNA2	-0.2443	7.74	7.58	7.5	7.34	7.2	7.02	7.1	6.58	6.49	6.19	6.23	6.1
U251 U7	MORC2 sgRNA1	-1.3205	7.97	7.75	7.13	7.03								
U251 U7	MORC2 sgRNA2	-1.3205	8.04	7.44	7.25	7.5								
U251 U7	SUV39H1 sgRNA1	-1.1116	3.05	1.54	2.94	2.61								
U251 U7	SUV39H1 sgRNA2	-1.1116	3.2	3.24	3.09	3.54								
U251 U7	CUL1 sgRNA1	-0.3767	3.93	3.71	3.56	4.19								
U251 U7	CUL1 sgRNA2	-0.3767	2.43	1.96	1.97	1.88								
U251 U7	GSK3B sgRNA1	-0.2266	5.94	5.75	5.88	5.49								
U251 U7	GSK3B sgRNA2	-0.2266	6.22	5.85	5.88	5.91								
U251 U7	SKP1 sgRNA1	-0.0153	13.1	14.4	13.9	15.1								
U251 U7	SKP1 sgRNA2	-0.0153	13.4	12.6	12.6	11.6								
U251 U7	CNOT8 sgRNA1	1.0027	2.06	2.15	1.91	2.1								
U251 U7	CNOT8 sgRNA2	1.0027	7.75	6.82	6.78	5.92								
U251 U7	PARN sgRNA1	1.0393	12.2	11.1	11.7	11								
U251 U7	PARN sgRNA2	1.0393	5.78	5.66	5.43	4.88								
U251 U7	CENPH sgRNA1	2.1881	3.73	3.66	3.56	3.72								
U251 U7	CENPH sgRNA2	2.1881	2.42	2.67	2.43	2.41								
U251 U7	CERS4 sgRNA1	2.4173	3.64	3.49	3.49	3.45								
U251 U7	CERS4 sgRNA2	2.4173	4.48	4.14	3.8	4.14								
U251 U7	GGNBP2 sgRNA1	3.0529	28.6	28.1	27.8	27.9								
U251 U7	GGNBP2 sgRNA2	3.0529	28.6	27	28.3	28.7								
U251 U7	WDR26 sgRNA1	3.2627	13.2	12.9	13.5	12.9								
U251 U7	WDR26 sgRNA2	3.2627	12	12.6	11.5	11.5								
U251 U7	INTS10 sgRNA1	3.2976	14.9	15.7	14.8	15.2								
U251 U7	INTS10 sgRNA2	3.2976	16.3	16.1	16.1	15.2								
U251 U7	ZBTB14 sgRNA1	4.7700	9.17	8.71	7.82	8.25								
U251 U7	ZBTB14 sgRNA2	4.7700	* virus prep and transductions for this experiment demonstrated bacterial contamination, excluded from analysis*											
U251 U7	CNOT11 sgRNA1	4.8411	15.8	15.7	15.2	16.6								
U251 U7	CNOT11 sgRNA2	4.8411	9.82	10.5	9.99	8.69								
U251 U7	RMND5A sgRNA1	4.8568	9.79	8.79	8.3	9.01								
U251 U7	RMND5A sgRNA2	4.8568	7.17	7.8	7.25	6.95								

(Continued on next page)

Table 1. Continued

Cell Line	Gene sgRNA	SLIDER Z	Replicates by Flow Cytometry, %GFP OE gated at 5% using LacZ sgRNA1											
			Sample 1	Sample 2	Sample 3	Sample 4	Sample 5	Sample 6	Sample 7	Sample 8	Sample 9	Sample 10	Sample 11	Sample 12
U251 U7	TSC2 sgRNA1	5.1805	12.4	11.2	11.7	10.9								
U251 U7	TSC2 sgRNA2	5.1805	7.2	7.14	6.66	7.32								
U251 U7	ATG9A sgRNA1	5.3687	9.39	9.7	10	9.58								
U251 U7	ATG9A sgRNA2	5.3687	4.55	4.82	4.86	4.67								
U251 U7	YPEL5 sgRNA1	5.4951	11.4	12	12.1	12.4								
U251 U7	YPEL5 sgRNA2	5.4951	13.2	13.7	14.1	12.9								
U251 U7	TSC1 sgRNA1	5.5131	11.7	12.2	11.7	12.9								
U251 U7	TSC1 sgRNA2	5.5131	9.6	9.45	9.35	9.61								
U251 U7	ATF7IP sgRNA1	6.2464	5.76	5.77	5.65	5.5								
U251 U7	ATF7IP sgRNA2	6.2464	3.57	3.33	3.18	3.49								
U251 U7	TRIM28 sgRNA1	6.2484	5.82	5.58	5.7	5.48								
U251 U7	TRIM28 sgRNA2	6.2484	6.69	6.21	6.11	6.36								
U251 U7	UBE2H sgRNA1	6.3129	35	34.9	32.5	33.2								
U251 U7	UBE2H sgRNA2	6.3129	12.9	13	12.4	12.6								
U251 U7	SETDB1 sgRNA1	6.4616	15.8	15.5	16	15.6								
U251 U7	SETDB1 sgRNA2	6.4616	21.1	21.2	21	20.7								
U251 U7	CNOT1 sgRNA1	7.8476	14.1	13.4	13.8	13.5								
U251 U7	CNOT1 sgRNA2	7.8476	14.4	14.2	14.5	13.5								

per subnetwork (Figure 3F). Inspection of the genes in each cluster revealed a negative regulatory network that consists of autophagy effectors, the GID/CTLH3 E3 ligase, the CNOT mRNA deadenylation complex, the KAP1 epigenetic corepressor complex, the SP1 transcription factor network, and genes involved in phospholipase- γ signaling downstream of immune cell receptors. WebGestalt (Figure S5E) and Enrichr (Figure S5F) both identified Leptin-Insulin Overlap, Nanoparticle Triggered Autophagy, PI3K-AKT-mTOR Signaling, and Neurodegeneration with Brain Iron Accumulation as enriched pathways.

Inspection of SLIDER scores for the 28 genes forming a network in STRING revealed differences between cell lines (Table 2). While genes in the CNOT network have uniformly high SLIDER scores across all three cell lines, members of the Autophagy and GID/CTLH clusters scored higher in MCF10A and U251 than in RWPE replicates. The SP1 and Immune Receptor Phospholipase Signaling genes are nominated primarily by high SLIDER scores in U251 replicates. Members of the Kap1-corepressor complex scored highly in MCF10A and RWPE but not in U251 cells, which is consistent with *ATF7IP* and *TRIM28* not validating by flow cytometry in U251 Clone 7 (Figure 3D). These differences suggest that negative regulation of *TRIM24* is governed by different process between cell types.

Review of the genes nominated by SLIDER revealed the unexpected outcome of *TRIM28* being nominated as a candidate negative regulator. *TRIM28* heterodimerizing with *TRIM24* was previously shown to protect *TRIM24* from SPOP-mediated degradation by the ubiquitin proteasome, establishing an SPOP-dependent post-translational mechanism for *TRIM28* as positive regulator of the *TRIM24* protein.¹⁸ Another unexpected outcome is that the screen did not nominate *SPOP* despite several studies establishing its role as a negative regulator of the *TRIM24* protein.^{3,16,18} This is despite MCF10A cells demonstrating enrichment of *SPOP* targeting sgRNA when sorted with a 15.8% GFP+ sorting gate in proof-of-principle experiments performed with a 6-sgRNA pool (Figure S2H). This suggests that while *SPOP* is active in this cell line, the MCF10A genome-wide screen with a 10% sorting gate was not sensitive enough to capture its role as a regulator. Owing to NGS readout failure of MCF10A replicates screened at a 20% sorting gate, we do not know if a more permissive gate would have nominated *SPOP* in MCF10A cells. Screening replicates performed with 10% and 20% GFP sorting gates in RWPE and U251 cells did not, suggesting *SPOP* may not be active in these two cell lines.

To further probe these observations, the cell lines screened were characterized for expression of *TRIM24*, *TRIM28*, and *SPOP* proteins (Figures 4A–4D). *TRIM24* is a 116.8 kDa protein that consistently resolved on 4–12% gradient gels as a band slightly above the 130kDa marker in the fluorescently labeled protein ladder used for western blots in this study (Figures 1, 4, and 5). MCF10A cells transduced with shRNA targeting *TRIM24* or an Empty Vector control showed that RNA-interference attenuated this band on membranes probed with two different *TRIM24* antibodies (Figures 4A and 4B), confirming that it is *TRIM24*. Cell lines used in our CRISPR screen demonstrate comparable *TRIM28* protein expression to the castration resistant prostate cancer cell line PC3, where *SPOP* activity has been characterized and endogenous protein expression of *TRIM24*, *TRIM28*, and *SPOP* has been reported.^{18,24} In contrast, *SPOP* protein was not detected by western blot in MCF10A, U251, or RWPE cells despite successful detection in whole cell lysate of PC3 cells (Figure 4D). The absence of an *SPOP* band in untransduced HEK293T cells is an expected result for this negative control cell line (see AbCam tech specs). These findings demonstrate that the cell lines used in this study do not express the *SPOP* protein at levels detectable by western blot, providing an explanation for why *SPOP* was not nominated.

The mechanism elucidated for *TRIM28* as a post-translational positive regulator of the *TRIM24* protein is *SPOP*-dependent.¹⁸ Cells without detectable levels of the *SPOP* protein therefore lack a dependency for positive post-translational *TRIM24* regulation by *TRIM28*. As observed, this is true for all three cell lines used in the CRISPR/Cas9 screen (Figure 4D). In contrast, experiments that developed the mechanism for positive post-translational regulation of the *TRIM24* protein by *TRIM28* focused on *SPOP* wild-type prostate cancer cells.¹⁸ It is noteworthy that there is no overlap between cell lines used in the study by Fong et al. and this study. Although RWPE cells are a prostate epithelial cell line, they were not used in the study by Fong et al. and also demonstrate no detectable expression of *SPOP* protein by western blot (Figure 4D). We surmise that this biological difference between cell lines is why the genome-wide CRISPR/Cas9 screen performed did not reflect the *SPOP*-dependent post-translational positive regulation of *TRIM24* by *TRIM28* reported by Fong et al.¹⁸

TRIM28 is known to interact with many proteins, form several protein complexes, and participate in the functions of those complexes.²⁵ This includes its well-established role as a member of the Kap1-corepressor

Table 2. SLIDER scores for genes in network identified using STRING and the top 150 candidate negative regulators nominated by CRISPR/Cas9 Screen, related to Figure 3F

Network Complex	Rank by SLIDER Score	Gene Name	MCF10A C6 10pct	RWPE C3 10pct	RWPE C3 20pct	RWPE C7 20pct	U251 C7 10pct	U251 C7 20pct	U251 C8 20pct	SLIDER Z	p value	FDR
KAP1	2	SETDB1	3.3475	2.9986	3.3337	3.7248	2.6283	-1.1931	2.2561	6.4616	1.0357E-10	4.6747E-07
	4	TRIM28	2.7847	3.5212	3.4605	3.3841	1.2434	0.9951	1.1427	6.2484	4.1466E-10	1.0835E-06
	5	ATF7IP	3.4144	2.5954	2.4535	3.0611	3.0417	1.6638	0.2964	6.2464	4.2011E-10	1.0835E-06
GID/CTLH	3	UBE2H	3.0749	-1.2690	3.3147	3.4607	3.8440	3.0418	1.2352	6.3129	2.7388E-10	9.8892E-07
	7	YPEL5	3.5508	0.5035	1.4819	1.3551	3.8310	3.8837	-0.0674	5.4951	3.9056E-08	3.2051E-05
	11	RMND5A	2.6201	0.6072	1.6208	1.6491	1.1102	2.3755	2.8669	4.8568	1.1931E-06	5.8217E-04
	29	MAEA	3.4570	0.3383	0.5502	1.9343	0.8476	2.7801	0.9729	4.1124	3.9153E-05	7.2279E-03
	61	AXIN1	-0.1454	2.9090	-1.4717	0.5748	2.2762	2.6364	2.8641	3.6449	2.6753E-04	2.6393E-02
	121	WDR26	3.5094	-2.6046	-0.0833	1.6559	3.5800	0.1844	2.3906	3.2627	1.1035E-03	5.8426E-02
CNOT	1	CNOT1	3.3089	3.5506	2.1077	2.7949	3.9997	3.2630	1.7380	7.8476	4.2412E-15	2.5524E-11
	12	CNOT11	3.2866	2.3365	0.4114	-0.4250	3.2576	2.8975	1.0439	4.8411	1.2909E-06	6.1333E-04
	143	YTHDF2	0.5290	1.6946	1.6929	1.9827	-0.0708	0.8412	1.7564	3.1848	1.4488E-03	6.7761E-02
AUTOPHAGY	6	TSC1	3.3238	0.8402	0.3794	3.0779	1.9771	1.9907	2.9971	5.5131	3.5260E-08	3.0313E-05
	8	ATG9A	3.0145	0.9398	1.5745	1.0705	2.9795	1.5305	3.0950	5.3687	7.9290E-08	5.9646E-05
	10	TSC2	3.7289	1.5458	-0.6705	3.1821	3.1100	-0.1801	2.9901	5.1805	2.2131E-07	1.3778E-04
	40	RB1CC1	2.9010	0.1311	0.4312	1.4377	2.1108	2.6456	0.6011	3.8774	1.0558E-04	1.3616E-02
	45	ULK1	2.6672	-0.9334	0.7642	2.3190	2.8366	2.4749	0.0527	3.8481	1.1903E-04	1.4138E-02
	117	ATG12	2.4783	0.6921	-0.7188	2.5373	3.1979	1.8690	-1.3892	3.2757	1.0541E-03	5.7147E-02
PHOSPHOLIPASE & IMMUNE RECEPTORS	148	C12orf44 (alias: ATG101)	2.6890	1.9426	-0.1488	-0.5170	1.5221	2.2445	0.6594	3.1718	1.5151E-03	6.9601E-02
	50	IPMK	-0.1252	2.7231	1.8880	2.4624	2.8189	1.4506	-1.1867	3.7914	1.4980E-04	1.6687E-02
	68	BLNK	1.7754	0.8474	0.7307	0.4935	1.1859	2.0575	2.4167	3.5934	3.2641E-04	2.8887E-02
	80	JAK2	1.0704	-0.7239	1.8073	2.4399	0.2682	1.7344	2.6377	3.4901	4.8277E-04	3.6317E-02
	131	PLCG1	-0.0092	0.0791	-0.2510	1.0108	3.1037	1.8351	2.7671	3.2262	1.2547E-03	6.1755E-02
	132	SOCS1	3.0517	0.7397	-0.6747	1.1014	1.5580	3.2045	-0.4471	3.2254	1.2580E-03	6.1755E-02
SP1	140	IGLL5	1.9365	1.8664	0.6231	0.4595	0.7604	2.4727	0.3330	3.1944	1.4014E-03	6.6756E-02
	62	SP1	0.0302	1.6874	1.6641	3.0347	2.3470	1.9822	-1.1437	3.6292	2.8435E-04	2.7468E-02
	111	JUNB	-1.9210	0.9139	2.3991	2.9263	-0.1366	1.3051	3.2380	3.2977	9.7491E-04	5.4629E-02
	136	ARNT	-0.2679	-1.4669	0.1483	3.2003	2.9330	0.7241	3.2128	3.2065	1.3434E-03	6.4849E-02

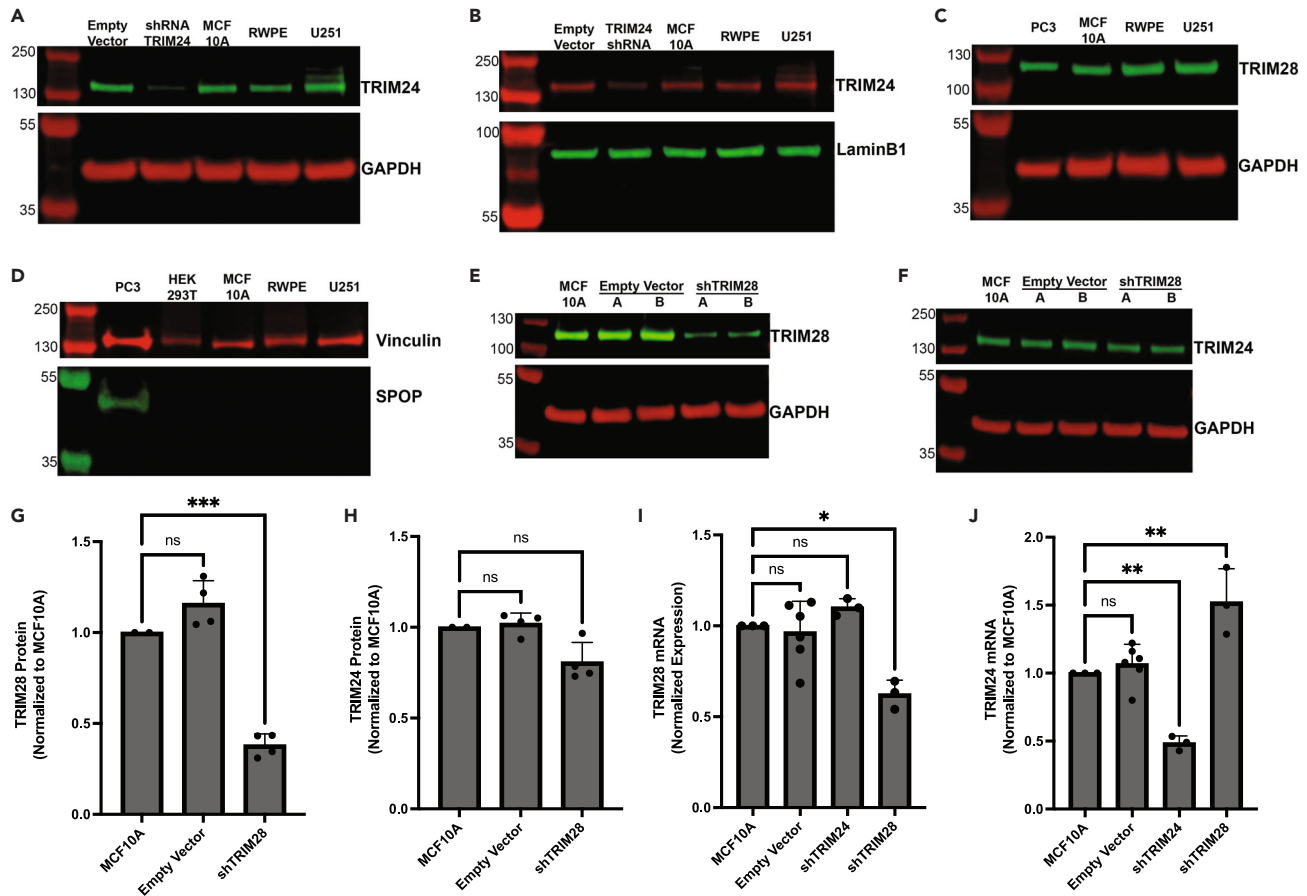


Figure 4. Screened cell lines lack SPOP protein expression and demonstrate negative regulation of TRIM24 mRNA expression by TRIM28

Replicate western blots for TRIM24 protein expression in MCF10A, RWPE, and U251 with lysates of MCF10A cells transfected with Empty Vector or shRNA targeting *TRIM24* included as controls for identification of TRIM24.

(A) Probed with rabbit anti-TRIM24 and mouse anti-GAPDH as a loading control.

(B) Probed with mouse anti-TRIM24 and rabbit anti-LaminB1 as a loading control. Both westerns (A,B) demonstrate migration of TRIM24 above the 130kDa marker in the PageRuler Plus ladder in 4–12% Bis-Tris NuPage gradient gels (see STAR Methods).

(C) Western blot comparing PC3, MCF10A, RWPE, and U251 cells for protein expression of TRIM28 using GAPDH as a loading control.

(D) Western blot comparing PC3, MCF10A, RWPE, and U251 cells for expression of SPOP protein using Vinculin as a loading control. PC3 lysate included as a positive control and lysate of untransduced HEK293T cells included as a negative control per antibody manufacturer’s specifications.

(E and G) Western blot assessing attenuation of TRIM28 by shRNA in two independent transductions of MCF10A cells. Lysates from paired Empty Vector transfected and untransduced MCF10A cells included as negative controls. Assayed in duplicate (see Data S4) to permit quantification and comparison.

(F and H) Western blot assessing effect of TRIM28 attenuation by shRNA on TRIM24 protein expression using the same lysates as shown in panel E. Assayed in duplicate to permit quantification and comparison (see Data S4).

(I) qRT-PCR quantification of *TRIM28* mRNA expression in shTRIM24, shTRIM28, and Empty Vector transfected MCF10A cells normalized to untransduced MCF10A cells as a control. Empty Vector and shRNA targeting *TRIM24* had no significant effect on *TRIM28* mRNA. shRNA targeting of *TRIM28* had the expected result of a decrease in *TRIM28* transcript.

(J) qRT-PCR quantification of *TRIM24* mRNA expression in shTRIM24, shTRIM28, and Empty Vector transfected MCF10A cells normalized to untransduced MCF10A cells as a control. Empty Vector had no significant effect on *TRIM24* mRNA. shRNA targeting *TRIM24* had the expected result of a decrease in *TRIM24* transcript. Cells with shRNA targeting *TRIM28* demonstrate increased *TRIM24* mRNA, consistent with negative regulation of *TRIM24* expression by *TRIM28*. (G–J) Statistical significance determined using Student’s t test for comparisons. p values: * <0.05 , ** <0.01 .

complex, a known negative regulator of gene expression.^{26,27} Three members of this complex (*TRIM28*, *SETDB1*, and *ATF7IP*) were nominated by SLIDER (Figures 3B and 3G) with high scores in RWPE and MCF10A cells (Table 2). To test whether *TRIM28* negatively regulates *TRIM24* expression, MCF10A cells were transfected with shRNA targeting *TRIM28* or an Empty Vector control. Western blot and qPCR assays demonstrate successful attenuation of *TRIM28* by shRNA without significant effects from transduction alone as assayed using Empty Vector controls (Figures 4E, 4G, and 4I). MCF10A cells with shRNA attenuating *TRIM28* do not show a significant change in TRIM24 protein, suggesting that TRIM28 is not as potent at

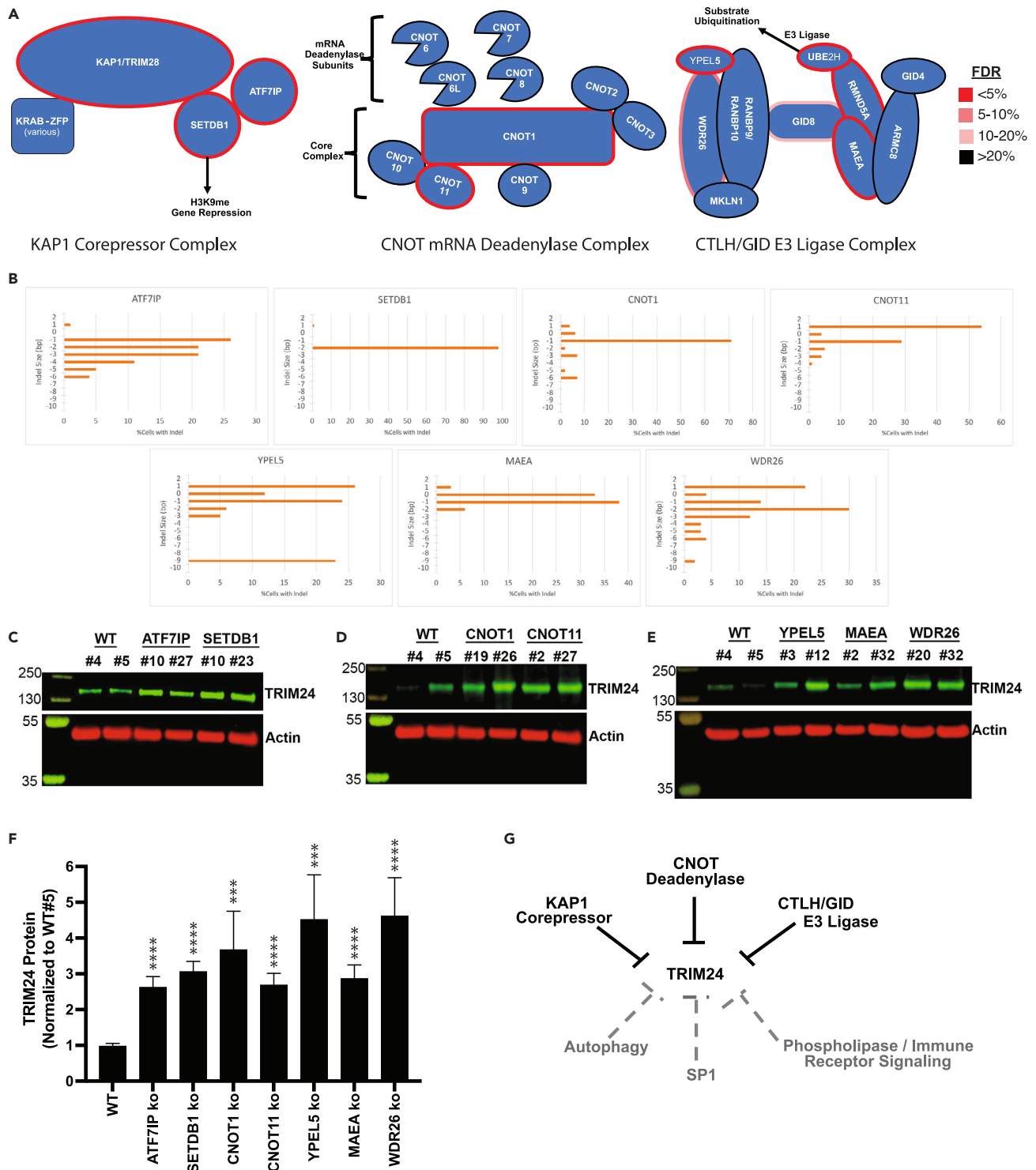


Figure 5. Validation of protein complexes in TRIM24's network of negative regulators

(A) Protein complexes known to suppress genes found in the negative regulatory network gleaned from STRING. Complex members are highlighted by their false discover rate (FDR) in our screen.

(B) Histograms of indel sizes resolved by ICE analysis of Sanger traces generated by Synthego on CRISPR/Cas9 edited MCF10A cell pools made to knockout individual members of the protein complexes highlighted in Panel A. Negative indel sizes indicate a deletion, positive indel sizes indicate an insertion, and

Figure 5. Continued

indel sizes that are not multiples of 3 are out-of-frame edits expected to confer functional gene knockout. Knockout is further characterized in individual clones expanded from these pools (see [Figure S7](#)).

(C) Western blot comparing TRIM24 protein expression in 2-clones/gene with knockout of genes that are members of the Kap1-corepressor complex to 2 clonally expanded WT-MCF10A clones as unedited controls.

(D) Western blot comparing TRIM24 protein expression in 2-clones/gene with knockout of genes that are members of the CNOT complex to 2 WT-clones as unedited controls.

(E) Western blot comparing TRIM24 protein expression in 2-clones/gene with knockout of genes that are members of the GID/CTLH complex to 2 WT-clones as unedited controls. C-E) Membranes were probed for Actin as a loading control. Westerns were repeated to and quantified using software for the LiCor Odyssey-Fc (see [Data S4](#)).

(F) Quantitative comparison of TRIM24 protein expression in clones with a knockout of a candidate regulator to TRIM24 protein expression in WT clones as unedited controls. TRIM24 protein was Actin normalized for loading and standardized to expression in WT clone #5 to permit comparison across western blots. Statistical significance determined by ANOVA and Student's t-tests for pairwise comparisons of normalized TRIM24 protein in clones with a specific gene knockout to WT controls. p value: ***<0.001, ****<1e-4.

(G) Model diagram for negative regulation of TRIM24 with solid black lines representing network components validated in this study. Dashed gray lines represent nominated cellular processes and effectors not validated in this study.

SPOP-dependent post-translational positive regulation of the TRIM24 protein in this cell line ([Figures 4F and 4H](#)). As explained above, this is likely because of undetectable expression of the SPOP protein that the mechanism depends on ([Figure 4D](#)). However, attenuation of *TRIM28* did result in a significant increase in *TRIM24* mRNA expression as observed in qRT-PCR assays ([Figure 4J](#)). These results do not challenge the Fong et al. study establishing *TRIM28* as an SPOP-dependent post-translational positive regulator of the TRIM24 protein. The data suggest that *TRIM28* can also negatively regulate *TRIM24* expression.

In this study, we further validate the three protein complexes nominated by network analysis using STRING ([Figure 3F](#)). These complexes are the KAP1-corepressor which suppresses gene expression,^{26,27} the CNOT deadenylase which post-transcriptionally suppresses genes,^{28,29} and the GID/CTLH E3-ligase which negatively regulates proteins by ubiquitination^{30–33} ([Figure 5A](#)). To validate these complexes as negative regulators of *TRIM24*, we chose 2–3 genes per complex to knockout in wild-type (WT) MCF10A cells. For the KAP1-corepressor complex we chose *SETDB1* and *ATF7IP*, which are necessary for the complex to suppress genes by histone methylation.^{27,34} For CNOT we chose *CNOT1* and *CNOT11*, which form the core of the complex^{28,29} and are not functionally compensated for by redundancy like CNOT's deadenylating subunits.^{35,36} For GID/CTLH we chose *YPEL5* and *WDR26* given recent evidence of a coordinated role for the two in substrate recruitment³³ and *MAEA* for its established role as a dependency for ubiquitination by the complex.^{31,32}

Knockouts were generated by Synthego Corporation using CRISPR/Cas9 to establish an MCF10A knockout pool for each gene. Adequate editing was confirmed by Synthego using ICE analysis of Sanger-sequenced genomic DNA amplicons to resolve the indels introduced by CRISPR/Cas9 near the start codon of targeted genes.³⁷ This analysis shows that the majority of cells in each knockout pool harbor out-of-frame indels in the form of 1 base pair (bp) insertions or deletions of 1, 2, 4, or 5 bps ([Figure 5B](#)). Resolution of indels with a size of 0 bp indicates that some cells were either not edited or harbor mono-allelic edits by Cas9. Individual clones expanded from each pool were therefore assayed to verify that the clones grew from an edited cell ([Figure S7](#)). We were not successful at identifying an antibody sensitive enough to resolve *ATF7IP* and *SETDB1* protein in whole cell lysates of WT-MCF10A cells. This is despite *SETDB1* targeting having a significant effect on TRIM24-mClover3 expression as assayed by flow cytometry ([Figure 3D](#)). We therefore confirmed the presence of indels in knockout clones established for these two genes using T7E1 assays ([Figures S7A and S7B](#)). Western blot analysis of knockout clones established for the other five genes demonstrated loss of protein expression for the targeted gene and in some cases destabilization of interacting complex members when compared to two WT-MCF10A clones expanded from single cells as unedited controls ([Figures S7C–S7G](#)). Clone #19 for *CNOT1* ([Figure S7C](#)), Clone #2 for *MAEA* ([Figure S7E](#)) and Clone #36 for *WDR26* ([Figure S7F](#)) demonstrate diminished but not abolished expression of the target, which would be expected for a clone with monoallelic knockout.

Attenuation of *TRIM28* by shRNA diminished but did not abolish TRIM28 protein ([Figures 4E and 4G](#)) and resulted in no significant change in TRIM24 protein despite an observed significant increase in *TRIM24* mRNA ([Figures 4F, 4H, and 4J](#)). Clones with knockout of either *ATF7IP* or *SETDB1*, genes encoding for partners of TRIM28 in the Kap1-corepressor complex, demonstrate a statistically significant 2- to 4-fold increase in TRIM24 protein expression by western blot when compared to WT control clones ([Figures 5C](#)

and 5F). These results further support a role for the Kap1-corepressor complex as a negative regulator of *TRIM24* expression.

Clones with loss of CNOT complex members demonstrate a statistically significant 2.5- to 5-fold increase in *TRIM24* protein compared to WT clones (Figures 5D and 5F). Assayed clones with knockout of GID/CTLH complex members demonstrate a statistically significant 3- to 5-fold increase in *TRIM24* protein compared to WT controls (Figures 5E and 5F). MAEA Clone #2 retaining partial expression of MAEA protein (Figure S7G) suggests this clone is not a biallelic knockout and may explain why MAEA editing did not show the same magnitude of *TRIM24* protein overexpression as knockouts of other GID/CTLH complex members (Figures 5E and 5F). WDR26 Clone #32 similarly shows diminished expression of WDR26 protein that suggests mono-allelic knockout while Clone #20 shows abolished WDR26 expression (Figure S7F). This difference may explain variability in the magnitude of *TRIM24* protein expression changes observed in WDR26 knockouts (Figures 5E and 5F). Likewise, *CNOT1* Clone #19 shows signs of monoallelic knockout (Figure S7C) and has a more modest increase in *TRIM24* protein expression than observed in Clone #26 (Figure 5D). Our prior work² showed that a 2- to 3-fold increase in *TRIM24* was sufficient to cause spontaneous tumorigenesis in murine mammary glands. Together, the results of these knockout experiments validate half of the negative regulatory network identified by our screen (Figure 5G) and demonstrate that genetic loss impairing any one of these complexes is sufficient to cause a biologically relevant increase in *TRIM24* expression.

Published work on components of the KAP1-corepressor,^{38,39} CNOT complex,^{29,40} and GID/CTLH complex^{31,41} demonstrate that silencing these genes impairs cellular proliferation and clonogenic survival. This motivated us to more formally assess whether the members of these complexes are essential using DepMap.⁴² Gene effect scores in DepMap are designed such that the median of known non-essential genes has a score of 0 and known common essential genes have -1 for a median score.⁴³ Therefore, genes with a negative score are likely to play an essential role in cellular proliferation and survival. Across the 1070 cell lines screened in DepMap, all three members of the KAP1 corepressor, 9 of 10 CNOT complex members, and 9 of 10 GID/CTLH complex members have gene-effect scores that are significantly less than 0 (Figure S6A). Given these results, we would not expect many tumors to have deletions or mutations leading to loss of function at these genes. Of interest, analysis on cBioportal^{15,44} shows that 15.2% of invasive breast carcinomas and 15.9% of prostate adenocarcinomas analyzed by TCGA harbor mutations, deletions, or structural variants in at least one of these genes (Figures S6B and S6C). In contrast, deletions and mutations at these genes are scant in TCGA profiles of glioblastoma (Figure S6D).

DISCUSSION

In this study, we present a screen for negative regulators of *TRIM24* that is specific enough for 93% of tested candidates with an FDR < 10% to validate, sensitive enough to nominate 220 candidates at this threshold, and informative enough to detect a regulatory network among its hits. These discoveries exceed what a single study can validate and will serve as a resource for further research on *TRIM24*.

The performance achieved by our screen lends credibility to the platform we've developed. By avoiding overexpression from an ectopic construct, our screen remained sensitive to regulators that cause modest, ~2- to 5-fold changes in expression. Complexes validated from our screen demonstrate the inclusive nature of endogenous tags, capturing regulation by epigenetic, post-transcriptional, and post-translational effectors. Our analytical approach also allowed us to extract more insight than popular counts-based methods like MAGeK and DrugZ, which both underperformed SLIDER in precision recall analysis.

The proliferation of CRISPR screens has inspired many new scoring systems. What makes SLIDER unique is the use of statistical models that account for the consequences of sorting on guide populations. MAUDE is a recent algorithm that accomplishes this by inferring the effect each guide has on a reporter's signal from screening data gathered using multiple sorting gates per sample.⁴⁵ Screens like ours that use a single gate and an unsorted control are not compatible with MAUDE despite being a more common study design. SLIDER therefore addresses an unmet need for an algorithm appropriate for the many screens conducted to study gene and process regulation using one sorting gate screen and an unsorted control.

We initiated our screen to better understand how *TRIM24* becomes overexpressed in human solid tumors. Independent patient cohorts assessed by IHC demonstrate *TRIM24* overexpression in 45–70% of breast

carcinomas,^{10,13} 5–25% of prostate adenocarcinomas,^{3,6} and about 35–70% of glioblastomas.^{4,9} The most recurrently deleted gene amongst members of the complexes we have validated is *CNOT7*, a deadenylase subunit which is known to be buffered by orthologue redundancy from *CNOT8*.^{35,40} It is not surprising that deletions and mutations in the genes for these complexes are rare given our DepMap analysis finding 21 of 23 tend toward essentiality. In a heterogeneous tumor, neoplastic cells with loss of function of an essential complex will drop out of the population because of natural selection. We therefore surmise that loss of negative regulation by deleterious genetic events affecting these three complexes is an explanation that leaves many cases of *TRIM24* overexpressing tumors unaccounted for. Alternative explanations such as loss of other negative regulators nominated by but not validated in this study or gain of function events leading to positive regulation of *TRIM24* merit further exploration.

Prior studies firmly establish a role for *SPOP* as a negative regulator of the *TRIM24* protein in prostate cancer, where mutations of *SPOP* are known to promote oncogenesis.^{3,16,18} In an elegant study, Fong et al.¹⁸ demonstrate a wild-type *SPOP* dependent mechanism for *TRIM28* to function as a post-translational positive regulator of the *TRIM24* protein through heterodimerization. Our screen missed *SPOP*-mediated regulation, including positive post-translational regulation of *TRIM24* by *TRIM28* that is dependent on *SPOP*, owing to our cell lines not expressing detectable levels of the *SPOP* protein. Unexpectedly, we also learned that *TRIM28* and the Kap1-corepressor complex negatively regulate *TRIM24* expression. Biology is rife with examples of proteins that regulate expression of a gene in one manner while post-translationally regulating the expressed protein product in another. For example, p53 is an MDM2-dependant negative post-translational regulator of the p21 protein that also positively regulates expression of the *CDKN1A* gene encoding for p21.⁴⁶ Our screen is also not the only study to find an upstream regulator that affects *TRIM24* expression differently than it does *TRIM24* protein stability. In response to DNA damage, ATM-kinase increases *TRIM24* expression in a p53-dependant manner while also negatively regulating the *TRIM24* protein post-translationally by phosphorylating serine residues that promote its proteolysis.¹⁷ We therefore do not see negative regulation of *TRIM24* expression by *TRIM28* to be in conflict with *SPOP*-dependent post-translational positive regulation of the *TRIM24* protein by *TRIM28*. These roles can co-exist.

The Kap1-corepressor is one of three complexes we validated as negative regulators of *TRIM24*. Regulation by *CNOT* and the *GID/CTLH* complex suggest new directions for *TRIM24* research. *WDR26* haploinsufficiency syndrome,⁴⁷ loss of the *MAEA* gene in Wolf-Hirschhorn Syndrome^{48,49} and microdeletion of the locus encoding *GID4* in Smith-Magenis syndrome⁵⁰ each represent human genetic disorders with impairment of the *GID/CTLH* complex. Deleterious heterozygous and *de novo* mutations in *CNOT1* are also associated with holoprosencephaly⁵¹ and Vissers-Bodmer syndrome.⁵² Our findings suggest *TRIM24* would be overexpressed in these genetic disorders. Determination of cancer predisposition in patients with these syndromes is confounded by small sample size due the disorders being rare. Of interest, all five phenotypically converge on complications in neurodevelopment. Insertional mutagenesis in *Drosophila melanogaster* leading to loss of function in the *TRIM24* homologue *bonus* results in flies with extra neurons, suggesting a functional role for *bonus* in neurodevelopment.^{53,54} Meanwhile, *TRIM24*'s role in mammalian neurodevelopment remains uncharted.

Other components of the *TRIM24* regulatory network we've elucidated will similarly inspire studies of *TRIM24* function in previously unexplored contexts. For instance, *TRIM24*'s function in the context of autophagy and phospholipase signaling are also uncharted research topics. While developing the relationship between these two pathways and *TRIM24* is beyond the scope of this study, *TRIM24* being downregulated by either raises questions about why these pathways would attenuate *TRIM24*. SLIDER scores from the screen in this study also suggest there are variances between cell lines with respect to how much these pathways influence *TRIM24* expression, providing an initial framework for developing studies that further probe context specific relationships between the pathways and *TRIM24*.

Finally, *TRIM24* is one of many understudied genes. Absent a clear context in which to formulate hypotheses, it can be difficult to unravel the roles that understudied genes play in biology and disease. The screening platform we developed using SLIDER, endogenous fluorescent protein tagging, and FACS elucidated a regulatory network upstream of *TRIM24* in a single study. This advance is transferable to the study of any gene and should facilitate efforts to develop informed contexts in which to probe the regulation of understudied genes at-large.

Limitations of the study

The study elucidates a network of protein complexes that suppress *TRIM24* but does not develop the underlying biochemistry by which each complex acts on *TRIM24* and its gene products. Benchmarking of SLIDER is limited in this study to its performance when scoring for enrichment by sorting. Further evaluation is needed to determine its utility for studies identifying candidates on the basis of depletion by sorting. This limitation prevents this study from identifying positive regulators of *TRIM24* from the CRISPR/Cas9 screen performed. The network identified by SLIDER and STRING is generated from an *in vitro* screen and is not assayed using *in vivo* models. The cell lines and culture conditions used for the screen also do not capture all contexts in which *TRIM24* is regulated. This includes missing regulation by effectors with an SPOP-dependent mechanism and those with functions specific to conditions of DNA-damage.

STAR★METHODS

Detailed methods are provided in the online version of this paper and include the following:

- KEY RESOURCES TABLE
- RESOURCE AVAILABILITY
 - Lead contact
 - Materials availability
 - Data and code availability
- EXPERIMENTAL MODEL AND STUDY PARTICIPANT DETAILS
 - Cell lines
- METHOD DETAILS
 - sgRNA design
 - sgRNA cloning
 - Molecular cloning of mClover3 donor vector for HITI
 - Knock-in of mClover3 to *TRIM24*
 - Flow cytometry and FACS
 - Droplet digital PCR
 - Junction spanning PCR and sanger sequencing of integration
 - Whole cell lysate for western blot
 - PAGE and western blotting
 - shRNA knockdowns
 - qRT-PCR
 - Cell fractionation
 - Cyclohexamide chase
 - Lentiviral CRISPR knockouts and CRISPR activation
 - Virus prep, transduction of TKOv3, and expansion of cells for FACS screen
 - sgRNA readouts of screenability controls
 - NGS of plasmid pool and screened cells
 - Analysis of CRISPR screen readouts
 - SLIDER
 - Precision recall analysis comparing SLIDER to drugZ and MAGeCK
 - Analysis of published screens
 - Commercially obtained CRISPR knockout pools
- QUANTIFICATION AND STATISTICAL ANALYSIS

SUPPLEMENTAL INFORMATION

Supplemental information can be found online at <https://doi.org/10.1016/j.isci.2023.107126>.

ACKNOWLEDGMENTS

We thank the Lozano-lab for sharing lab space and providing valuable input. This study was supported by National Institutes of Health grant RO1 CA214871 and a research award from the Emerson Collective to MCB. LRP was funded by the John J Kopchick fellowship and by the National Center for Advancing Translational Sciences of the National Institutes of Health under Award Numbers TL1TR003169 and UL1TR003167. Sequencing was performed at MD Anderson Cancer Center Science Park Next-Generation Sequencing Facility supported by Cancer Prevention and Research Institute of Texas Core

Facility Support Grants (RP120348 and RP170002). The Flow Cytometry and Cell Imaging Core shared resource is partially funded by the National Cancer Institutes Cancer Center Support Grant P30CA16672.

AUTHOR CONTRIBUTIONS

Conceptualization: L.R.P. and M.C.B.; Methodology: L.R.P., M.M., S.A.S., and K.A.; Software: L.R.P.; Validation: L.R.P., S.A.S., M.M., P.K., K.A., A.L.R., and D.B.; Formal Analysis: L.R.P. and S.A.S.; Investigation: L.R.P., S.A.S., M.M., P.K., K.A., A.L.R., and D.B.; Resources: M.C.B. and G.T.H.; Data Curation: L.R.P. and M.M.; Writing – Original Draft: L.R.P.; Writing – Reviewing and Editing: M.C.B., G.T.H., L.R.P., and S.A.S.; Visualization: L.R.P., S.A.S., and K.A.; Supervision: M.C.B. and G.T.H.; Project Administration: L.R.P. and M.C.B.; Funding Acquisition: M.C.B., G.T.H., and L.R.P.

DECLARATION OF INTERESTS

The authors declare no competing interests.

INCLUSION AND DIVERSITY

We support inclusive, diverse, equitable conduct of research.

Received: August 10, 2022

Revised: March 12, 2023

Accepted: June 9, 2023

Published: June 14, 2023

REFERENCES

- Pathiraja, T.N., Thakkar, K.N., Jiang, S., Stratton, S., Liu, Z., Gagea, M., Shi, X., Shah, P.K., Phan, L., Lee, M.H., et al. (2015). TRIM24 links glucose metabolism with transformation of human mammary epithelial cells. *Oncogene* 34, 2836–2845. <https://doi.org/10.1038/onc.2014.220>.
- Shah, V.V., Duncan, A.D., Jiang, S., Stratton, S.A., Allton, K.L., Yam, C., Jain, A., Krause, P.M., Lu, Y., Cai, S., et al. (2021). Mammary-specific expression of Trim24 establishes a mouse model of human metaplastic breast cancer. *Nat. Commun.* 12, 5389. <https://doi.org/10.1038/s41467-021-25650-z>.
- Groner, A.C., Cato, L., de Tribolet-Hardy, J., Bernasocchi, T., Janouskova, H., Melchers, D., Houtman, R., Cato, A.C.B., Tschopp, P., Gu, L., et al. (2016). TRIM24 Is an Oncogenic Transcriptional Activator in Prostate Cancer. *Cancer Cell* 29, 846–858. <https://doi.org/10.1016/j.ccell.2016.04.012>.
- Zhang, L.H., Yin, A.A., Cheng, J.X., Huang, H.Y., Li, X.M., Zhang, Y.Q., Han, N., and Zhang, X. (2015). TRIM24 promotes glioma progression and enhances chemoresistance through activation of the PI3K/Akt signaling pathway. *Oncogene* 34, 600–610. <https://doi.org/10.1038/onc.2013.593>.
- Cui, Z., Cao, W., Li, J., Song, X., Mao, L., and Chen, W. (2013). TRIM24 overexpression is common in locally advanced head and neck squamous cell carcinoma and correlates with aggressive malignant phenotypes. *PLoS One* 8, e63887. <https://doi.org/10.1371/journal.pone.0063887>.
- Höflmayer, D., Fraune, C., Hube-Magg, C., Simon, R., Schroeder, C., Büscheck, F., Möller, K., Dum, D., Weidemann, S., Wittmer, C., et al. (2021). Overexpression of the TRIM24 E3 Ubiquitin Ligase is Linked to Genetic Instability and Predicts Unfavorable Prognosis in Prostate Cancer. *Appl. Immunohistochem. Mol. Morphol.* 29, e29–e38. <https://doi.org/10.1097/PAI.0000000000000901>.
- Li, H., Sun, L., Tang, Z., Fu, L., Xu, Y., Li, Z., Luo, W., Qiu, X., and Wang, E. (2012). Overexpression of TRIM24 correlates with tumor progression in non-small cell lung cancer. *PLoS One* 7, e37657. <https://doi.org/10.1371/journal.pone.0037657>.
- Liu, X., Huang, Y., Yang, D., Li, X., Liang, J., Lin, L., Zhang, M., Zhong, K., Liang, B., and Li, J. (2014). Overexpression of TRIM24 is associated with the onset and progress of human hepatocellular carcinoma. *PLoS One* 9, e85462. <https://doi.org/10.1371/journal.pone.0085462>.
- Lv, D., Li, Y., Zhang, W., Alvarez, A.A., Song, L., Tang, J., Gao, W.Q., Hu, B., Cheng, S.Y., and Feng, H. (2017). TRIM24 is an oncogenic transcriptional co-activator of STAT3 in glioblastoma. *Nat. Commun.* 8, 1454. <https://doi.org/10.1038/s41467-017-01731-w>.
- Ma, L., Yuan, L., An, J., Barton, M.C., Zhang, Q., and Liu, Z. (2016). Histone H3 lysine 23 acetylation is associated with oncogene TRIM24 expression and a poor prognosis in breast cancer. *Tumour Biol.* 37, 14803–14812. <https://doi.org/10.1007/s13277-016-5344-z>.
- Miao, Z.F., Wang, Z.N., Zhao, T.T., Xu, Y.Y., Wu, J.H., Liu, X.Y., Xu, H., You, Y., and Xu, H.M. (2015). TRIM24 is upregulated in human gastric cancer and promotes gastric cancer cell growth and chemoresistance. *Virchows Arch.* 466, 525–532. <https://doi.org/10.1007/s00428-015-1737-4>.
- Offermann, A., Roth, D., Hupe, M.C., Hohensteiner, S., Becker, F., Joerg, V., Carlsson, J., Kuempers, C., Ribbat-Idel, J., Tharun, L., et al. (2019). TRIM24 as an independent prognostic biomarker for prostate cancer. *Urol. Oncol.* 37, 576.e1–576.e10. <https://doi.org/10.1016/j.urolonc.2019.05.006>.
- Tsai, W.W., Wang, Z., Yiu, T.T., Akdemir, K.C., Xia, W., Winter, S., Tsai, C.Y., Shi, X., Schwarzer, D., Plunkett, W., et al. (2010). TRIM24 links a non-canonical histone signature to breast cancer. *Nature* 468, 927–932. <https://doi.org/10.1038/nature09542>.
- Wang, F.Q., Han, Y., Yao, W., and Yu, J. (2017). Prognostic relevance of tripartite motif containing 24 expression in colorectal cancer. *Pathol. Res. Pract.* 213, 1271–1275. <https://doi.org/10.1016/j.prp.2017.08.008>.
- Cerami, E., Gao, J., Dogrusoz, U., Gross, B.E., Sumer, S.O., Aksoy, B.A., Jacobsen, A., Byrne, C.J., Heuer, M.L., Larsson, E., et al. (2012). The cBio cancer genomics portal: an open platform for exploring multidimensional cancer genomics data. *Cancer Discov.* 2, 401–404. <https://doi.org/10.1158/2159-8290.CD-12-0095>.
- Theurillat, J.P.P., Udeshi, N.D., Errington, W.J., Svinkina, T., Baca, S.C., Pop, M., Wild, P.J., Blattner, M., Groner, A.C., Rubin, M.A., et al. (2014). Prostate cancer. Ubiquitylome analysis identifies dysregulation of effector substrates in SPOP-mutant prostate cancer. *Science* 346, 85–89. <https://doi.org/10.1126/science.1250255>.
- Jain, A.K., Allton, K., Duncan, A.D., and Barton, M.C. (2014). TRIM24 is a p53-induced E3-ubiquitin ligase that undergoes

- ATM-mediated phosphorylation and autodegradation during DNA damage. *Mol. Cell Biol.* 34, 2695–2709. <https://doi.org/10.1128/MCB.01705-12>.
18. Fong, K.W., Zhao, J.C., Song, B., Zheng, B., and Yu, J. (2018). TRIM28 protects TRIM24 from SPOP-mediated degradation and promotes prostate cancer progression. *Nat. Commun.* 9, 5007. <https://doi.org/10.1038/s41467-018-07475-5>.
 19. Bajar, B.T., Wang, E.S., Lam, A.J., Kim, B.B., Jacobs, C.L., Howe, E.S., Davidson, M.W., Lin, M.Z., and Chu, J. (2016). Improving brightness and photostability of green and red fluorescent proteins for live cell imaging and FRET reporting. *Sci. Rep.* 6, 20889. <https://doi.org/10.1038/srep20889>.
 20. Gonatopoulos-Pourmatzis, T., Wu, M., Braunschweig, U., Roth, J., Han, H., Best, A.J., Raj, B., Aregger, M., O'Hanlon, D., Ellis, J.D., et al. (2018). Genome-wide CRISPR-Cas9 Interrogation of Splicing Networks Reveals a Mechanism for Recognition of Autism-Misregulated Neuronal Microexons. *Mol. Cell.* 72, 510–524.e12. <https://doi.org/10.1016/j.molcel.2018.10.008>.
 21. Popa, S., Villeneuve, J., Stewart, S., Perez Garcia, E., Petrunkina Harrison, A., and Moreau, K. (2019). Genome-wide CRISPR screening identifies new regulators of glycoprotein secretion. *Wellcome Open Res.* 4, 119. <https://doi.org/10.12688/wellcomeopenres.15232.2>.
 22. Simeonov, D.R., Gowen, B.G., Boontanart, M., Roth, T.L., Gagnon, J.D., Mumbach, M.R., Satpathy, A.T., Lee, Y., Bray, N.L., Chan, A.Y., et al. (2017). Discovery of stimulation-responsive immune enhancers with CRISPR activation. *Nature* 549, 111–115. <https://doi.org/10.1038/nature23875>.
 23. Timms, R.T., Menzies, S.A., Tchasovnikarova, I.A., Christensen, L.C., Williamson, J.C., Antrobus, R., Dougan, G., Ellgaard, L., and Lehner, P.J. (2016). Genetic dissection of mammalian ERAD through comparative haploid and CRISPR forward genetic screens. *Nat. Commun.* 7, 11786. <https://doi.org/10.1038/ncomms11786>.
 24. Wang, D., Ma, J., Botuyan, M.V., Cui, G., Yan, Y., Ding, D., Zhou, Y., Krueger, E.W., Pei, J., Wu, X., et al. (2021). ATM-phosphorylated SPOP contributes to 53BP1 exclusion from chromatin during DNA replication. *Sci. Adv.* 7, eabd9208. <https://doi.org/10.1126/sciadv.abd9208>.
 25. Czerwińska, P., Mazurek, S., and Wiznerowicz, M. (2017). The complexity of TRIM28 contribution to cancer. *J. Biomed. Sci.* 24, 63. <https://doi.org/10.1186/s12929-017-0374-4>.
 26. Friedman, J.R., Fredericks, W.J., Jensen, D.E., Speicher, D.W., Huang, X.P., Neilson, E.G., and Rauscher, F.J., 3rd (1996). KAP-1, a novel corepressor for the highly conserved KRAB repression domain. *Genes Dev.* 10, 2067–2078. <https://doi.org/10.1101/gad.10.16.2067>.
 27. Sripathy, S.P., Stevens, J., and Schultz, D.C. (2006). The KAP1 corepressor functions to coordinate the assembly of de novo HP1-demarcated microenvironments of heterochromatin required for KRAB zinc finger protein-mediated transcriptional repression. *Mol. Cell Biol.* 26, 8623–8638. <https://doi.org/10.1128/MCB.00487-06>.
 28. Collart, M.A., and Panasenko, O.O. (2012). The Ccr4–not complex. *Gene* 492, 42–53. <https://doi.org/10.1016/j.gene.2011.09.033>.
 29. Shirai, Y.T., Suzuki, T., Morita, M., Takahashi, A., and Yamamoto, T. (2014). Multifunctional roles of the mammalian CCR4–NOT complex in physiological phenomena. *Front. Genet.* 5, 286. <https://doi.org/10.3389/fgene.2014.00286>.
 30. Huffman, N., Palmieri, D., and Coppola, V. (2019). The CTLH Complex in Cancer Cell Plasticity. *JAMA Oncol.* 2019, 4216750. <https://doi.org/10.1155/2019/4216750>.
 31. Lampert, F., Stafa, D., Goga, A., Soste, M.V., Gilberto, S., Olieric, N., Picotti, P., Stoffel, M., and Peter, M. (2018). The multi-subunit GID/CTLH E3 ubiquitin ligase promotes cell proliferation and targets the transcription factor Hbp1 for degradation. *Elife* 7, e35528. <https://doi.org/10.7554/eLife.35528>.
 32. Maitland, M.E.R., Onea, G., Chiasson, C.A., Wang, X., Ma, J., Moor, S.E., Barber, K.R., Lajoie, G.A., Shaw, G.S., and Schild-Poulter, C. (2019). The mammalian CTLH complex is an E3 ubiquitin ligase that targets its subunit myosin for degradation. *Sci. Rep.* 9, 9864. <https://doi.org/10.1038/s41598-019-46279-5>.
 33. Sherpa, D., Chrustowicz, J., Qiao, S., Langlois, C.R., Hehl, L.A., Gottmukkala, K.V., Hansen, F.M., Karayel, O., von Gronau, S., Prabu, J.R., et al. (2021). GID E3 ligase supramolecular chelate assembly configures multipronged ubiquitin targeting of an oligomeric metabolic enzyme. *Mol. Cell.* 81, 2445–2459.e13. <https://doi.org/10.1016/j.molcel.2021.03.025>.
 34. Schultz, D.C., Ayyanathan, K., Negorev, D., Maul, G.G., and Rauscher, F.J., 3rd (2002). SETDB1: a novel KAP-1-associated histone H3, lysine 9-specific methyltransferase that contributes to HP1-mediated silencing of euchromatic genes by KRAB zinc-finger proteins. *Genes Dev.* 16, 919–932. <https://doi.org/10.1101/gad.973302>.
 35. Dede, M., McLaughlin, M., Kim, E., and Hart, T. (2020). Multiplex enCas12a screens detect functional buffering among paralogs otherwise masked in monogenic Cas9 knockout screens. *Genome Biol.* 21, 262. <https://doi.org/10.1186/s13059-020-02173-2>.
 36. Mostafa, D., Takahashi, A., Yanagiya, A., Yamaguchi, T., Abe, T., Kureha, T., Kuba, K., Kanegae, Y., Furuta, Y., Yamamoto, T., and Suzuki, T. (2020). Essential functions of the CNOT7/8 catalytic subunits of the CCR4–NOT complex in mRNA regulation and cell viability. *RNA Biol.* 17, 403–416. <https://doi.org/10.1080/15476286.2019.1709747>.
 37. Conant, D., Hsiau, T., Rossi, N., Oki, J., Maures, T., Waite, K., Yang, J., Joshi, S., Kelso, R., Holden, K., et al. (2022). Inference of CRISPR Edits from Sanger Trace Data. *CRISPR J* 5, 123–130. <https://doi.org/10.1089/crispr.2021.0113>.
 38. Spyropoulou, A., Gargalionis, A., Dalagiorgou, G., Adamopoulos, C., Papavassiliou, K.A., Lea, R.W., Piperi, C., and Papavassiliou, A.G. (2014). Role of histone lysine methyltransferases SUV39H1 and SETDB1 in gliomagenesis: modulation of cell proliferation, migration, and colony formation. *NeuroMolecular Med.* 16, 70–82. <https://doi.org/10.1007/s12017-013-8254-x>.
 39. Sun, Y., Wei, M., Ren, S.C., Chen, R., Xu, W.D., Wang, F.B., Lu, J., Shen, J., Yu, Y.W., Hou, J.G., et al. (2014). Histone methyltransferase SETDB1 is required for prostate cancer cell proliferation, migration and invasion. *Asian J. Androl.* 16, 319–324. <https://doi.org/10.4103/1008-682X.122812>.
 40. Aslam, A., Mittal, S., Koch, F., Andrau, J.C., and Winkler, G.S. (2009). The Ccr4–NOT deadenylase subunits CNOT7 and CNOT8 have overlapping roles and modulate cell proliferation. *Mol. Biol. Cell* 20, 3840–3850. <https://doi.org/10.1091/mbc.e09-02-0146>.
 41. Wei, Q., Pinho, S., Dong, S., Pierce, H., Li, H., Nakahara, F., Xu, J., Xu, C., Boulais, P.E., Zhang, D., et al. (2021). MAEA is an E3 ubiquitin ligase promoting autophagy and maintenance of haematopoietic stem cells. *Nat. Commun.* 12, 2522. <https://doi.org/10.1038/s41467-021-22749-1>.
 42. Tsherniak, A., Vazquez, F., Montgomery, P.G., Weir, B.A., Kryukov, G., Cowley, G.S., Gill, S., Harrington, W.F., Pantel, S., Krill-Burger, J.M., et al. (2017). Defining a Cancer Dependency Map. *Cell* 170, 564–576.e16. <https://doi.org/10.1016/j.cell.2017.06.010>.
 43. Dempster, J.M., Boyle, I., Vazquez, F., Root, D.E., Boehm, J.S., Hahn, W.C., Tsherniak, A., and McFarland, J.M. (2021). Chronos: a cell population dynamics model of CRISPR experiments that improves inference of gene fitness effects. *Genome Biol.* 22, 343. <https://doi.org/10.1186/s13059-021-02540-7>.
 44. Gao, J., Aksoy, B.A., Dogrusoz, U., Dresdner, G., Gross, B., Sumer, S.O., Sun, Y., Jacobsen, A., Sinha, R., Larsson, E., et al. (2013). Integrative analysis of complex cancer genomics and clinical profiles using the cBioPortal. *Sci. Signal.* 6, pii. <https://doi.org/10.1126/scisignal.2004088>.
 45. de Boer, C.G., Ray, J.P., Hacohen, N., and Regev, A. (2020). MAUDE: inferring expression changes in sorting-based CRISPR screens. *Genome Biol.* 21, 134. <https://doi.org/10.1186/s13059-020-02046-8>.
 46. Enge, M., Bao, W., Hedström, E., Jackson, S.P., Moumen, A., and Selivanova, G. (2009). MDM2-dependent downregulation of p21 and hnRNP K provides a switch between apoptosis and growth arrest induced by pharmacologically activated p53. *Cancer Cell* 15, 171–183. <https://doi.org/10.1016/j.ccr.2009.01.019>.
 47. Skraban, C.M., Wells, C.F., Markose, P., Cho, M.T., Nesbitt, A.I., Au, P.Y.B., Begtrup, A., Bernat, J.A., Bird, L.M., Cao, K., et al. (2017). WDR26 Haploinsufficiency Causes a Recognizable Syndrome of Intellectual Disability, Seizures, Abnormal Gait, and Distinctive Facial Features. *Am. J. Hum. Genet.*

- Genet. 101, 139–148. <https://doi.org/10.1016/j.ajhg.2017.06.002>.
48. Yang, W.X., Pan, H., Li, L., Wu, H.R., Wang, S.T., Bao, X.H., Jiang, Y.W., and Qi, Y. (2016). Analyses of Genotypes and Phenotypes of Ten Chinese Patients with Wolf-Hirschhorn Syndrome by Multiplex Ligation-dependent Probe Amplification and Array Comparative Genomic Hybridization. *Chin. Med. J.* 129, 672–678. <https://doi.org/10.4103/0366-6999.177996>.
 49. Zollino, M., Orteschi, D., Rüter, M., Pfundt, R., Steindl, K., Cafiero, C., Ricciardi, S., Contaldo, I., Chieffo, D., Ranalli, D., et al. (2014). Unusual 4p16.3 deletions suggest an additional chromosome region for the Wolf-Hirschhorn syndrome-associated seizures disorder. *Epilepsia* 55, 849–857. <https://doi.org/10.1111/epi.12617>.
 50. Poisson, A., Nicolas, A., Cochat, P., Sanlaville, D., Rigard, C., de Leersnyder, H., Franco, P., Des Portes, V., Ederly, P., and Demily, C. (2015). Behavioral disturbance and treatment strategies in Smith-Magenis syndrome. *Orphanet J. Rare Dis.* 10, 111. <https://doi.org/10.1186/s13023-015-0330-x>.
 51. Kruszka, P., Berger, S.I., Weiss, K., Everson, J.L., Martinez, A.F., Hong, S., Anyane-Yeboah, K., Lipinski, R.J., and Muenke, M. (2019). A CCR4-NOT Transcription Complex, Subunit 1, CNOT1, Variant Associated with Holoprosencephaly. *Am. J. Hum. Genet.* 104, 990–993. <https://doi.org/10.1016/j.ajhg.2019.03.017>.
 52. Vissers, L.E.L.M., Kalvakuri, S., de Boer, E., Geuer, S., Oud, M., van Outersterp, I., Kwint, M., Witmond, M., Kersten, S., Polla, D.L., et al. (2020). De Novo Variants in CNOT1, a Central Component of the CCR4-NOT Complex Involved in Gene Expression and RNA and Protein Stability, Cause Neurodevelopmental Delay. *Am. J. Hum. Genet.* 107, 164–172. <https://doi.org/10.1016/j.ajhg.2020.05.017>.
 53. Salzberg, A., Prokopenko, S.N., He, Y., Tsai, P., Pál, M., Maróy, P., Glover, D.M., Deák, P., and Bellen, H.J. (1997). P-element insertion alleles of essential genes on the third chromosome of *Drosophila melanogaster*: mutations affecting embryonic PNS development. *Genetics* 147, 1723–1741. <https://doi.org/10.1093/genetics/147.4.1723>.
 54. Beckstead, R., Ortiz, J.A., Sanchez, C., Prokopenko, S.N., Chambon, P., Losson, R., and Bellen, H.J. (2001). Bonus, a *Drosophila* homolog of TIF1 proteins, interacts with nuclear receptors and can inhibit betaFTZ-F1-dependent transcription. *Mol. Cell.* 7, 753–765. [https://doi.org/10.1016/s1097-2765\(01\)00220-9](https://doi.org/10.1016/s1097-2765(01)00220-9).
 55. Li, W., Xu, H., Xiao, T., Cong, L., Love, M.I., Zhang, F., Irizarry, R.A., Liu, J.S., Brown, M., and Liu, X.S. (2014). MAGeCK enables robust identification of essential genes from genome-scale CRISPR/Cas9 knockout screens. *Genome Biol.* 15, 554. <https://doi.org/10.1186/s13059-014-0554-4>.
 56. Colic, M., Wang, G., Zimmermann, M., Mascal, K., McLaughlin, M., Bertolet, L., Lenoir, W.F., Moffat, J., Angers, S., Durocher, D., and Hart, T. (2019). Identifying chemogenetic interactions from CRISPR screens with drugZ. *Genome Med.* 11, 52. <https://doi.org/10.1186/s13073-019-0665-3>.
 57. Liao, Y., Wang, J., Jaehnig, E.J., Shi, Z., and Zhang, B. (2019). WebGestalt 2019: gene set analysis toolkit with revamped UIs and APIs. *Nucleic Acids Res.* 47, W199–W205. <https://doi.org/10.1093/nar/gkz401>.
 58. Xie, Z., Bailey, A., Kuleshov, M.V., Clarke, D.J.B., Evangelista, J.E., Jenkins, S.L., Lachmann, A., Wojciechowicz, M.L., Kropiwnicki, E., Jagodnik, K.M., et al. (2021). Gene Set Knowledge Discovery with Enrichr. *Curr. Protoc.* 1, e90. <https://doi.org/10.1002/cpz1.90>.
 59. Langmead, B., Trapnell, C., Pop, M., and Salzberg, S.L. (2009). Ultrafast and memory-efficient alignment of short DNA sequences to the human genome. *Genome Biol.* 10, R25. <https://doi.org/10.1186/gb-2009-10-3-r25>.
 60. Martin, M. (2011). Cutadapt removes adapter sequences from high-throughput sequencing reads. *EMBnet. j.* 17, 10–12. <https://doi.org/10.14806/ej.14817.14801.14200>.
 61. Concordet, J.P., and Haeussler, M. (2018). CRISPOR: intuitive guide selection for CRISPR/Cas9 genome editing experiments and screens. *Nucleic Acids Res.* 46, W242–W245. <https://doi.org/10.1093/nar/gky354>.

STAR★METHODS

KEY RESOURCES TABLE

REAGENT or RESOURCE	SOURCE	IDENTIFIER
Antibodies		
TRIM24, Rabbit	Proteintech	Cat # 14208-1-AP; RRID: AB_2256646
TRIM24, Mouse	Santa-Cruz	Cat# sc-271266; RRID: AB_10611751
TRIM28, Rabbit	AbCam	Cat# ab10483; RRID: AB_297222
SPOP, Rabbit	AbCam	Cat# ab137537
MCAF1 (alias ATF7IP), Rabbit	Abcam	Cat# ab84497; RRID: AB_1861009
MAEA, Rabbit	Proteintech	Cat# 15238-1-AP; RRID: AB_2137505
YPEL5, Rabbit	Proteintech	Cat# 11730-1-AP; RRID: AB_2217465
WDR26, Rabbit	Novus Biologicals	Cat# NBP1-83628; RRID: AB_11015693
CNOT1, Rabbit	Proteintech	Cat# 14276-1-AP; RRID: AB_10888627
CNOT1, Rabbit	Bethyl Laboratories	Cat# A305-787A-M; RRID: AB_2891683
CNOT11, Rabbit	Novus Biologicals	Cat# NBP2-55823
β-ACTIN, Mouse	Sigma-Aldrich	Cat# A5441; RRID: AB_476744
GAPDH, Mouse	Santa Cruz	Cat# sc32233; RRID: AB_627679
LaminB1, Rabbit	AbCam	Cat#: ab133741; RRID: AB_2616597
Vinculin, Mouse	AbCam	Cat# ab130007; RRID: AB_11156698
Goat Anti-Rabbit, AF800	Invitrogen	Cat# A32735
Goat Anti-Mouse, AF680	Invitrogen	Cat# A32729
Bacterial and virus strains		
Stbl3	Invitrogen	C404010
Top10	Invitrogen	C737303
Chemicals, peptides, and recombinant proteins		
keratinocyte serum free medium (KSFM) supplemented with EGF and Bovine Pituitary Extract	Gibco	17005-042
DMEM/F12	Gibco	11320-033
Horse Serum	Gibco	26050-088
Insulin	Gibco	12585-014
EGF	EMD Millipore	01-107
Hydrocortisone	Sigma	H0888
Cholera toxin	Sigma	9012-63-9
HEPES	Gibco	15630-080
MEM non-Essential Amino Acids	Gibco	11140-050
L-Glutamine	Gibco	G7513
Sodium Pyruvate	Gibco	S8636
Geneticin	Sigma	A1720
0.05% trypsin/0.53mM EDTA	Gibco	25300-054
FBS	Gibco	A31605
DMSO	Sigma	D8418
T4 PNK	NEB	M0201S
CutSmart Buffer	NEB	B7204
Esp3I	Thermo	ER0452

(Continued on next page)

Continued

REAGENT or RESOURCE	SOURCE	IDENTIFIER
EcoRI	NEB	R0101S
BamHI	NEB	R0136S
T4 Ligase	NEB	M0202S
XbaI	NEB	R0145S
HindIII	NEB	R0104S
Q5 Site Direct Mutagenesis Kit	NEB	E0554
Herculase II Polymerase	Agilent	600675
Clontech HD polymerase (alias: Advantage® HD Polymerase)	Takara	639241
DAPI	Sigma	D9542
DPBS	Gibco	14200-075
BSA	Sigma	A7906
2x ddPCR Supermix for Probes (No dUTP)	Biorad	1863024
Protease Inhibitor Cocktail	Milipore	539131
4X NuPAGE LDS sample buffer	Invitrogen	NP0007
PageRuler Plus protein ladder	Thermo Fisher	26619
TriZol	Invitrogen	15596-026
MES running buffer	Invitrogen	NP0002
4-12% NuPAGE Bis-Tris gradient gel	Invitrogen	NP0335BOX
0.45um nitrocellulose membrane	Bio-Rad	1620115
2X SYBR Green qPCR master mix	Bimake	B21203
Cyclohexamide	Sigma	C1988
40micron PES filter	Thermo	7232545
Lipofectamine 3000	Thermo	L3000008
500mL PES Stericups	Millipore	S2GPU05RE
Puromycin 10mg/mL	Sigma	P4512
AL buffer	Qiagen	19075
SPRI beads	Beckman Coulter	B23317
Amasa SE Nucleofection Kit	Lonza	V4XC-1012
Plasmid Miniprep Kit	IBI Scientific	IB47101
Maxi Prep Kit	Qiagen	12162
iScript cDNA synthesis kit	BioRad	1708891
Blood and Cell Culture DNA Mini Kit	Qiagen	13323
Blood and Cell Culture DNA Midi Kit	Qiagen	13343
DNA Clean and Concentrator 100	Zymo	D4029
PCR Product Purification kit	Qiagen	28104
EnGen® Mutation Detection Kit	NEB	E3321S
TOPO TA Cloning kit	Invitrogen	
BCA Protein Assay kit	Pierce	23225
Biological samples		
PC3 Cell Lysate	Santa-Cruz	sc-2220
Critical commercial assays		
RPP30 copy number assay, HEX probe	Biorad	dHsaCP2500350
shTRIM24	Dharmacon	V3LHS_16660
shTRIM28	Dharmacon	V3LHS_640072

(Continued on next page)

Continued

REAGENT or RESOURCE	SOURCE	IDENTIFIER
Deposited data		
Splicing reporter and Srrm4 regulation screens performed by FACS	Gonatopoulos-Pournatzis et al. ²⁰	GEO: GSE112599
Enhancer mapping by CRISPRa screens performed using FACS	Simeonov et al. ²²	GEO: GSE98178
Glycoprotein secretion screen performed by FACS	Popa et al. ²¹	GEO: GSE133692
ERAD regulation screens performed by FACS with stringent sorting	Timms et al. ²³	Data S2 of Timms et al. ²³
Experimental models: Cell lines		
Human: MCF10A	ATCC	CRL 10317
Human: U251	MD Anderson Brain Tumor Center	
Human: RWPE (alias: RWPE1)	kind gift from Dean Tang	
Human: HEK293FT	ThermoFisher	R70007
Oligonucleotides		
See table in supplemental information		
Recombinant DNA		
TKOv3 Library	Addgene	90294
pUC19	Addgene	50005
lentiCRISPRv2	Addgene	52961
pXPR_502	Addgene	96923
pNCS-mCLOver3	Addgene	74236
Software and algorithms		
SLIDER	This paper	https://github.com/LRPatel1/SLIDER https://doi.org/10.5281/zenodo.6902782
R	R Foundation for Statistical Computing	https://www.r-project.org Version 4.3.0
QuantaSoft Analysis Pro	BioRad	QuantaSoft AP
Prism	Dotmatics	https://www.graphpad.com Version 9.5.1
MAGeCK	Liu Lab, Dana Farber Cancer Center ⁵⁵	https://github.com/liulab-dfci/MAGeCK
DrugZ	Hart Lab, MD Anderson Cancer Center ⁵⁶	https://github.com/hart-lab/drugz
WebGestalt	Zhang Lab, Baylor College of Medicine ⁵⁷	http://www.webgestalt.org
Enrichr	Ma'ayan Lab, Mount Sinai School of Medicine ⁵⁸	https://maayanlab.cloud/Enrichr/
STRING	STRING Consortium 2023	https://string-db.org
Bowtie1	Salzberg Lab, Johns Hopkins University ⁵⁹	https://github.com/BenLangmead/bowtie
FASTQC	Barbraham Institute, Bioinformatics Group	https://github.com/s-andrews/FastQC
Cutadapt	Rahmann Lab, TU Dortmund University ⁶⁰	https://github.com/marcelm/cutadapt
FlowJo	BD Biosciences	https://www.flowjo.com/
GPP sgRNA designer	GPP Webportal, Broad Institute	https://portals.broadinstitute.org/gpp/public/analysis-tools/sgrna-design
CRISPOR	Haeussler Lab, UC Santa Cruz ⁶¹	http://crispor.tefor.net

RESOURCE AVAILABILITY

Lead contact

Further information and requests for resources should be directed to and will be fulfilled by the lead contact, Michelle C Barton (bartonsh@ohsu.edu).

Materials availability

Cell lines generated with in-frame knockin of *mClover3* to *TRIM24* will be shared by the [lead contact](#) upon request.

Data and code availability

- sgRNA counts, gene scores from SLIDER, and original western blot images are available in this paper's supplementary information. Flow cytometry reported in the paper will be shared by the [lead contact](#) upon request. NGS reads for CRISPR screens in this paper will be shared by the [lead contact](#) upon request.
- Original code has been deposited at GitHub and Zenodo and is publicly available as of the date of publication. Repository links and DOIs are listed in the [key resources table](#).
- Any additional information required to reanalyze the data reported in this paper is available from the [lead contact](#) upon request.

EXPERIMENTAL MODEL AND STUDY PARTICIPANT DETAILS

Cell lines

RWPE refers to RWPE1 cells that were a kind gift from Dean Tang and maintained in keratinocyte serum free medium (KSFM) supplemented with EGF and Bovine Pituitary Extract per manufacturer protocol (Gibco, 17005-042). U251 cells were obtained from the MD Anderson Brain Tumor Center and grown in DMEM/F12 supplemented with 10% fetal bovine serum. MCF10A cells were obtained from ATCC and cultured in DMEM/F12 supplemented with 5% horse serum, 10 ug/mL Insulin, 20ng/mL EGF, 0.5 ug/mL hydrocortisone, 100ng/mL cholera toxin, 10 mM HEPES, and 1mM calcium chloride. HEK293FT cells were obtained from Thermo/Fisher and grown in high glucose DMEM supplemented with 10% fetal bovine serum, 0.1mM Non-Essential Amino Acids, 6mM L-glutamine, 1mM Sodium Pyruvate, 500ug/mL Geneticin. Cells lines were validated by STR profiling performed by the MD Anderson Cell Line Core and routinely mycoplasma tested. Cultures were maintained using sterile technique without the use of antibiotics or antimycotics, grown at 37C and 5% CO₂ in water jacketed incubators in 10cm or 15cm plates to ~80% confluence, and passaged 1:12 for no more than 12 passages before reviving a low passage cryostock. Cells were collected by washing plates with Dulbecco's Modified Phosphate Buffered Saline (DPBS), treating with 1.5-3mL 0.05% trypsin/0.53mM EDTA, resuspending cells to a volume 10-15mL of neutralization buffer (1% FBS in DPBS), centrifuging at 500g for 6 minutes, and resuspending in DPBS or cell culture media for subculture or experiments. Frozen stocks were made at passages 3-5 by aliquoting 2-5 million cells per cryovial in cell culture media +10% DMSO and freezing at -80C using isopropanol filled cryocontainers. Stocks were transferred to liquid nitrogen within 48 hours of freezing for cryostorage.

METHOD DETAILS

sgRNA design

For use in HIT1, 200bp of genomic DNA sequence including 150bp upstream of the stop codon and 50bp downstream in exon 19 of *TRIM24* was obtain from UCSC genome browser and used for sgRNA design using tools at mit.crispr.edu to obtain sgRNA with high specificity. For efficacy, this list was filtered for guides also identified using The Broad Institute's GPP sgRNA designer for knockout guides. sgRNA were further selected after mapping their target sites using the UCSC Genome Browser to pick sgRNA upstream of the stop codon. The CRISPOR webtool was then used to select the guide with the least computationally predicted off-targets. For CRISPR activation and CRISPR knockout experiments, sgRNA were designed using the Broad Institute's GPP sgRNA designer. For single gene perturbation experiments validating the results of screening TKOv3, two sgRNA were selected per gene from the TKOv3 library, favoring sgRNA labeled as active by SLIDER's filtering step across independent screen replicates.

sgRNA cloning

sgRNA were ordered as oligo pairs (Sigma) with the following sequences: 5'-**CACCG**NNNNNNNNNNNNNNNNNNNNNNNN-3' and 5'-**AAAC**nnnnnnnnnnnnnnnnnnnnnnnn**C**-3'. Overhangs are in bold, NNN represents sgRNA sequence, nnn represents its reverse complement. Oligonucleotides were resuspended to 100uM, annealed and treated with T4 PNK (NEB) at 10uM in 10uL reactions, diluted 1:200, and ligated into Esp3I (Thermo) digested lentiCRISPRv2 (Addgene 52961) for viral CRISPR-knockout by Cas9 or Esp3I digested pXPR_502 (Addgene 96923) for viral CRISPR-activation by dCas9-VP64 using 1uL diluted oligo and 100-200ng digested vector in 20uL T4 ligase (NEB) reactions. Ligation reactions were transformed into Stbl3 (Invitrogen) and selected for colonies on Agar plates with 100ug/mL Ampicillin. Five colonies were grown overnight in 5mL LB suspension cultures with 100ug/mL Ampicillin, 4mL of each culture was miniprep (IBI Scientific), and Sanger sequenced using the U6f primer. The remaining 1mL of the culture was stored at -80 as a glycerol stock. The colony with highest yield among those with correct sgRNA sequence was retained and used.

Molecular cloning of mClover3 donor vector for HIT1

pUC19 (#50005) and pNCS-mClover3 (#74236) plasmids were obtained from Addgene, grown from colonies struck on Agar plates with 100ug/mL ampicillin, and miniprep (IBI) from 5mL cultures grown in LB with 100ug/mL ampicillin. pNCS-mClover3 was sequence confirmed T7fwd and T7rev primers. pUC19 was digested at 37C with EcoRI (NEB) and BamHI (NEB) in Cutsmart buffer (NEB) for 24hr using 2.5ug plasmid. Digested plasmid was purified by isopropanol precipitation followed by two washes with 70% ethanol and resuspension in sterile water. An mClover3 insert without its ATG start site and flanked with sgRNA target sites matching the guide selected for HIT1 were prepared for cloning into pUC19 by performing 20 cycles of PCR annealing for 10 sec at 67C, extension for 75 sec at 72C, and denaturing at 95C for 5sec in a 20uL reaction using mcloHITIF and mcloHITIR primers, 100ng of pNCS-mClover3 as template, and the Herculase II polymerase (Agilent). Amplicons were cleaned up using PCR product purification (Qiagen), digested in 50uL reactions overnight with EcoRI and BamHI in Cutsmart buffer at 37C, and cleaned up again using PCR product purification before ligation using a 3:1 molar ratio of insert to vector in 20uL T4 ligase (NEB) reactions per manufactures protocol. Ligations were transformed into Stbl3, selected on ampicillin plates, miniprep from 5 colonies and Sanger sequenced using M13fwd and M13rev primers. The colony with the highest yield and expected sequence was labeled pUC-mClov, preserved as a glycerol stock, and used for further cloning. The SV40 DNA targeting sequence was added to pUC-mClov by digesting the vector with XbaI and HindIII as described for pUC19 double digests above, annealing DTSfwd and DTSrev oligos before treating with T4 PNK (NEB) at 10uM in 10uL reactions as described for sgRNA cloning, and diluting the annealed PNK product 1:200 before using 1uL as insert with 100 ug of double digested pUC-mClov in 20uL T4 ligase reactions (NEB). Ligations were transformed into Stbl3, selected on ampicillin plates, miniprep from 5 colonies, and Sanger sequenced using M13fwd and M13rev primers. The colony with the highest yield and expected sequence was labeled pUC-mClov-DTS, preserved as a cryostock, and used to reappend TRIM24's C-terminal NLS peptide RKKRLKSIEER to the end of mClover3's ORF to assure knock-in products preserve this localization signal. This was accomplished by using NEB's Q5 Site Directed Mutagenesis Kit (E0554) per manufactures protocol and the primers Q5SDM_F and Q5SDM_R, which were designed using the webtool NEBaseChanger. Six clones were miniprep, Sanger sequenced using M13fwd and M13rev primers, and the colony with highest yield and the intended sequence was maxi prep as Donor Vector.

Knock-in of mClover3 to TRIM24

Chemically modified sgRNA targeting the sequence CTTTGGAGGCGTTTCTTCCG and recombinant Cas9 were ordered from Synthego Corporation (Redwood City, CA, USA) and assembled one hour before nucleofection into ribonucleoprotein complexes in a 25uL solution with 20 pmol Cas9 at a 9:1 sgRNA-to-Cas9 ratio per manufacturer's protocol. Knock-in was performed by nucleofecting 600,000 cells with 6.6uL of RNP and 2.5ug HIT1 Donor Vector in 100uL cuvettes using two cuvettes per cell line, the Amaxa 4D Nucleofector (Lonza), SE nucleofection kits (Lonza), and the Amaxa programs FF130, DS138, and DS126 for MCF10A, RWPE, and U251 cells, respectively. Nucleofected cells were recovered in prewarmed cell culture plates with fully supplemented media, exchanged of media after 12 hours to remove residual nucleofection reagents, and grown for 2 weeks before FACS for GFP+ cells to enrich expressive mClover3 integrants. Sorting was performed using gates drawn using auto-fluorescing parental cells for background of 1/100,000 live single cells. Enriched cells were expanded until 70% confluence was reached in 10cm plates before single cell sorting of GFP+ cells into 96-well plates to isolated knock-in clones. When clones were

expanded from 96well plates reached 70% confluence in a 6cm plate, a quarter of the cells were used for characterization by droplet digital PCR (ddPCR) and junction-spanning PCR assays and the remainder were preserved as cryostocks. Two clones per cell line with a single integration of mClover3 as a mono-allelic on-target knock-in were identified by ddPCR, expanded from frozen stocks, and used for all subsequent work.

Flow cytometry and FACS

Cells were trypsinized, collected, resuspended at a concentration of 1–5 million cells/mL in FACS buffer (DPBS, 2.5mM EDTA, 0.1% BSA, 3uM DAPI), and passed through a 40um before aliquoting into flow tubes or sterile non-adhesive 96-well plates. Flow cytometry was performed using an Agilent Novocytte 3000 in 96-well plate format for single gene perturbation studies and using 5mL flow tubes for characterization of mClover3-knockin clones. FACS was performed by the MD Anderson North Campus Flow Core using the BD FACSAria II. On both instruments, cells were gated using forward scatter (FSC) vs side scatter (SSC) plots, viable cells were gated for using DAPI vs FSC plots, and doublets were discriminated against using FSC-A vs FSC-H. GFP gating controls were drawn using untransduced HITI knock-in clones or parental cell lines without knock-in depending on the experiment. Data were exported as fcs files and imported into FlowJo for analysis and visualization. For single cell sorts, suspensions were prepared at 500,000–750,000 cells/mL, cells were sorted into prewarmed 96 well plate containing 200uL fully supplemented media per well, and plates with sorted cells were returned to a sterile incubator within a hour starting a sort. For genomescale FACS screens, batches of cells were collected, resuspended in sorting buffer at a concentration of 5 million cells per mL, 1mL was sample from each batch prepared and pooled to establish an unsorted control, and 5–6mL of the suspension was provided to the core for sorting. If a prior batch had not finished sorting, sorting was stopped and the new batch was started to prevent artifacts from sorting cells that loose GFP intensity or become stressed after an hour in suspension.

Droplet digital PCR

Three custom FAM probes were designed for copy number assays and ordered from Biorad (see below). Genomic DNA from HITI edited clones or parental cell lines was digested with HindIII and 100ng was used as template with 2x ddPCR Supermix (Biorad), 1uL FAM-probe, and 1uL HEX-probe, in 20uL reaction mix. Droplets were generated in DG8 cartridges using the QX200 Droplet Generator, transferred to 96 well PCR plates, sealed, and thermal cycled after activating polymerase for 1 min at 95C for 40 cycles of denaturation for 30sec at 94C and annealing/extension for 1 min at 55C followed by 10 min at 98C to deactivate enzyme and an overnight hold at 4C. Temperature changes during thermal cycling were ramped per manufacturer protocol. Droplets were read using the QX200 ddPCR System and analyzed using QuantaSoft. Data was imported into Prism for visualization. Error bars for ddPCR experiments are Poisson errors estimated from droplet variation. All assays were performed using 2 channels with RPP30 copy number assay using a HEX probe (Biorad: dHsaCP2500350) as an internal copy number control.

Junction spanning PCR and sanger sequencing of integration

200 ng of genomic DNA from clones generated by HITI or parental controls was used as template and amplified using Clontech HD polymerase and the primers 5JunctF and 3JunctR in 20uL reactions for 25 cycles of denaturation at 95C for 20sec, 30 sec annealing at 62C, and 1 minute of extension at 72C. PCR products were resolved on by ethidium bromide staining on 1.5–2% agarose gels with wild-type amplicons of an expected size of 146bp and successful knockins having an expected amplicon of 886bp. Knockin amplicons were excised, gel purified, and TOPO cloned using TOPO TA Cloning kits (Invitrogen). TOPO clones were sequenced using M13f, M13r, mClovSeqr, and mClovSeqf.

Whole cell lysate for western blot

Whole cell lysate was prepared by incubating cells in lysis buffer (50mM Tris-HCl, pH7.5; 150mM NaCl; 10mM EDTA; 10mM EGTA; 1% NP-40 (Igepal CA-630), 1% Triton-X 100, 1.5% SDS, with Protease Inhibitor Cocktail (Millepore, 539131) for 30 minutes on ice. Samples were sonicated at 20% duty cycle for five pulses at five seconds each on ice bath, then boiled for five minutes at 95°C. Lysates were centrifuged at 20,000g, 4°C, for 10 minutes. Supernatant transferred to new tube and total protein quantified on a FLUOstar Omega (BMG LABTECH) microplate reader, with BSA (bovine serum albumin) standards, using BCA Protein Assay kit (Pierce, 23225) per manufacturer recommendations. Whole cell lysates were boiled at 95°C for two minutes into 4X NuPAGE LDS sample buffer (Invitrogen, NP0007) before resolving proteins on a NuPAGE Bis-Tris gradient gel. PC3 lysate was obtained commercially from Santa-Cruz (sc-2220).

PAGE and western blotting

Protein samples (15–30 μ g total protein/lane) loaded onto 4–12% NuPAGE gels (Invitrogen, NP0335BOX) with MES running buffer (Invitrogen, NP0002) and with PageRuler Plus (Thermo Fisher, 26619) protein ladder loaded as needed. Gels run at room temperature, constant 160–170V for 40–70 minutes. Protein gels were wet transferred under moderate stirring with blotting buffer (25mM Tris, 192mM Glycine, 20% Methanol) at constant 380 mA, for 1.5–2 hours, onto 0.45 μ m nitrocellulose membrane (Bio-Rad, 1620115) at 4°C. Membranes placed in dark boxes, were subsequently blocked in 3% non-fat dry milk (w/v) with PBS-T (phosphate buffered saline with 0.2% Tween-20 (v/v)) blocking buffer and primary antibodies added for overnight binding at 4°C with gentle rocking. Membranes were washed with PBS-T (0.1% Tween-20(v/v)), three times for 10 minutes each wash, at room temperature with gentle rocking. Alexa Fluor conjugated secondary antibodies added into blocking buffer and membranes rocked at room temperature for two hours, followed by three water washes, five minutes each. Westerns imaged with LiCor Odyssey-Fc. Protein band intensity determined using the machine's software for analysis was normalized to loading control intensity within the same blot. Fold change in normalized TRIM24 relative to WT-MCF10A clones or untransduced MCF10A controls was determined by dividing the normalized TRIM24 value for a clone or transduced sample by the value for WT clone #5 for clones or by the untransduced MCF10A control assayed on the same blot.

shRNA knockdowns

shRNA knockdowns and empty vector control transductions were performed using pre-packaged and titered lentivirus generated from pGIPZ shRNA expression vectors by the MD Anderson functional genomics core. Transductions were performed in six well plates using 50000 MCF10A cells/well and virus at an MOI of 1. After overnight transduction, media was replaced and selection was begun 48 hours after transduction using puromycin at a concentration of 2 μ g/mL. After 2 days of selection cells were harvested and replated in a 10cm. When the culture reached 80% confluence (4–5d), cells were harvested with 10% of cells preserved in frozen stocks and the remaining cells used for RNA extraction and whole cell lysate preparation. TRIM24 shRNA was transduced one. Two independent transductions we performed of TRIM28 targeting shRNA. Each shRNA transduction was performed in parallel with a paired empty vector transduction. Hairpins used were V3LHS_16660 for TRIM24 and V3LHS_640072 for TRIM28 (Dharmacon).

qRT-PCR

RNA was extracted using TriZol (Invitrogen) and the RNeasy Mini kit with on-column DNase I digestion (Qiagen). cDNA was generated using the iScript cDNA synthesis kit (BioRad) and 1 μ g of RNA in 20 μ L reactions per manufacturers protocol. cDNA was diluted 1:20 and loaded at 1 μ L/well with gene specific primers in 10 μ L qRT-PCR reactions using 2X SYBR Green qPCR master mix (Bimake) per manufacturer's protocol. Amplifications was carried for 40 cycles with denaturation for 15sec at 95C, 10 sec annealing at 55C, and extension at 60C for 30 sec after 1min at 95C for hot-start. Plates were cycled, read, and analyzed on a CFX384 (BioRad). Gene expression was quantified relative to ATCB as a house keeping gene using the delta-Ct method and normalized to control samples using the delta-delta-Ct method.

Cell fractionation

2–4 million cells were collected, washed twice with DPBS, and resuspended in 225 μ L of hypotonic cell swelling buffer (10mM HEPES pH 7.7, 10mM KCl, 1.5mM MgCl₂, 0.1mM glycerol, 340mM sucrose). Once resuspended, 25 μ L of 10% triton was added to initiate cell lysis on ice for 10 minutes with brief mixing by inversion every 3–5 mins. Nuclei were pelleted by centrifugation at 1300g for 10 min at 4C and 225 μ L of supernatant was collected into a new tube. Nuclei were washed twice with 200 μ L hypotonic cell swelling buffer then resuspended in Nuclear Lysis Buffer (3mM EDTA, 0.2mM EGTA, 500 mM NaCl, 1mM DTT) for 30 min on ice with 5sec of vortexing every 5–6 mins. Chromatin was then pelleted at 20000g for 10 min at 4C and soluble nuclear lysate was collected and transferred to a new tube. Chromatin pellets were washed twice with Nuclear Lysis Buffer before resuspension in 200 μ L of whole cell lysis buffer, sonication with three 5sec pulses, and boiling at 98C for 5 min before centrifugation at 20000g for 10 min at 4C. The supernatant was collected as a chromatin lysate. All fractions were stored at –80C until further use. Buffers were freshly supplemented with protease inhibitors.

Cyclohexamide chase

750,000 cells were plated in ten 6cm dishes 36 hrs prior to cyclohexamide chase. Media was replaced in all plates with treatment media (cell culture media + 10 μ g/mL cyclohexamide) at the start of the chase and

every 2 hours during the chase. One plate was washed 2X with DPBS and treated with 300 μ L of whole cell lysis buffer at each time point. At 12 hrs of treatment, cells showed >20% cell death and the chase was stopped without collecting 12hr lysates. Cells were lysed in plates on ice for 5 min, scraped, collected in Eppendorf tubes, sonicated, boiled for five minutes, and cleared with centrifugation at 20000g for 5 min at 4C. Cleared lysates were transferred to new tubes and stored at -80°C until assayed by Western Blot. Lamin B was used as a loading control for these experiments instead of actin given its longer half-life and greater stability.

Lentiviral CRISPR knockouts and CRISPR activation

Virus for experiments using single guides and for screenability pools were packaged in 10cm dishes by growing 293FT cells to 60% confluence in fully supplemented media, changing media to DMEM/F12 with 1%FBS, and transfecting cells with 2.4 μg psPAX2, 1.6 μg pMD2G, and 4 μg of lentiCRISPRv2 or pXPR_502 plasmids for a total of 8 μg plasmid DNA using lipofectamine 3000. After 12 hours of transfection, media was changed to 8.0 mL virus collection media (DMEM + 1g/mL BSA, 1%FBS, 10mM HEPES pH7.9). After 48 hours of virus collection, media was collected, centrifuged at 500g for 10min to pellet debris, passed through a 40micron PES filter. Virus was used fresh or flash frozen in 2.5 mL aliquots until use. Transduction was performed by plating 1–2 million cells in 6cm plates, infection with 0.5-1mL virus for 36 hrs, then selecting with puromycin at a concentration of 1 $\mu\text{g}/\text{mL}$ for RWPE1 cells, 2 $\mu\text{g}/\text{mL}$ for MCF10A cells, and 1 $\mu\text{g}/\text{mL}$ for U251 cells. Puromycin concentrations were selected from kill curves for the lowest dose leading to 100% death at 48 hours of selection in untransduced parental cells of each line.

Virus prep, transduction of TKOv3, and expansion of cells for FACS screen

TKOv3 plasmid was obtained from the Hart lab. For TKOv3 library virus, packaging was performed using the same transfection time and ratios of psPAX2, pMD2G, and library plasmid as single gene or small pool experiments, but are scaled for transfection in 15 cm plates using 16 μg total DNA and lipofectamine 3000. Virus was made as a single batch for screens using twenty-five 15cm plates, each with 20mL of virus collection media. Virus was pooled and filtered using 500mL PES Stericups, aliquoted in 15mL tubes, and flash frozen until cells were transduced for the screen or for functional titers. To titer library virus, aliquots of 10 million cells were suspended in 20mL cell culture media in 50mL tubes and treated with 5mL library virus thawed to room temperature the same day. Cells with virus were then plated in a 15cm dish for 36hrs of transduction then collected and replated at 5million cells per plate into 2–4 plates with half of the plates receiving puromycin. After 48 hours of selection, cells were counted in each plate, MOI was determined from %survival, and used to estimate the amount of virus needed to infect 10 million cells at an MOI of 0.3. Library scale infections were carried out by scaling this estimate to infect 250–400 million cells at in 500mL suspensions aliquoted into 15cm plates. To measure the actual MOI achieved, one plate of the 25 transduced was split 1:6 and assayed similarly to viral titration. Library scale transductions achieved MOIs of 0.14–0.56, resulting in >500X coverage with $\geq 75\%$ singlet infection. To maintain uniformity, cells were collected from all plates used for transduction after 3 days of puromycin selection, pooled, counted, and replated in puromycin at 5–7 million cells (70-98X) per plate. Pooling was also performed at each passage. Cells for FACS screens with 10% sorting gates were expanded from transduction until the day of sorting. Sorting dates were determined by the availability of ~ 6 hr blocks on the BD FACSAria II at the MD Anderson North Campus Flow Core. The time between transduction and sorting appointments for these 3 replicates ranged from 16-24 days. C6 had the longest delay between transduction and sorting followed by R3. Reads for these two replicates demonstrate shorter and broader distributions from prolonged passaging when compared to U7, which was sorted on day 16 of selection (Figure S4C). For FACS sorts with 20% sorting gates, frozen stocks were made on day 7 of selection at 7.5 million cells/cryostock (105X), 6 stocks were revived and expanded in puromycin for 7–10 days before sorting, limiting the total time in culture to 14-17 days to limit the risk of missing genes because their sgRNA dropout or become so enriched before sorting that FACS cannot increase their rank enough to enable detection by SLIDER.

sgRNA readouts of screenability controls

Genomic DNA was extracted from Screenability Controls using the Blood and Cell Culture DNA Mini Kit (Qiagen) and from Genomewide CRISPR screens using the Blood and Cell Culture DNA Midi or Mini Kit depending on sorting yields. For Screenability controls, read outs were generated from 600ng of genomic DNA spread out over 3-50 μL reactions using ReadOut_f, the appropriate ReadOut_r primer for activation and knockout pools, and Herculanase II (Agilent). Instead of barcoding and generating an

NGS library, the PCR product obtained was TOPO cloned using the TOPO TA cloning kit (Invitrogen) and 25 colonies were miniprep and Sanger sequenced using M13f and M13r primers. sgRNA sequences were counted manually by inspecting Sanger reads and colonies with low quality reads were excluded from sgRNA counting.

NGS of plasmid pool and screened cells

Genomic DNA was extracted using AL buffer (Qiagen) for cell lysis followed by overnight isopropanol precipitation at -80°C . Precipitated DNA was washed three times with ice cold 70% ethanol and resuspended in DNase free water. DNA clumps were resolved by mechanical shearing with a 27-gauge insulin needle. For unsorted cells, 100ug of genomic DNA was used for sgRNA readout PCR in 32 reactions with a volume of 50uL each spread over 32 wells of a 96-well plate. For sorted cells, all of the genomic DNA obtained was used in 32 reactions at 50uL per well. For plasmid pool sequencing 500ng was used as template DNA spread over 10 reactions 50uL reactions. Read PCR products were pooled across wells and cleaned up from genomic DNA using DNA Clean and Concentrator 100 kits (Zymo) or from plasmid pool readouts using PCR Product Purification kits (Qiagen). Cleaned up PCR products were quantified by nanodrop and used at 100ng/rxn in twelve 50uL Herculase II reactions for NGS library generation in a second step PCR using an equimolar pool of staggered Step2_F primers and a barcoded LCV2_st2Rx primer, where x matches the i7 barcode chosen for the sample. Step2 PCR reactions were pooled cleaned up and size selected using (0.95,0.55) dual SPRI bead clean up, and submitted for sequencing on an Illumina NextSeq to a minimum depth of 40 million reads/sample. All readout and Step2 PCR reactions using Herculase II polymerase (Agilent) were performed in provided master mix per manufactures protocol. PCR cycles proceeded after a 3-minute start at 95C and ended with a 10 minute final elongation before holding at 4C. Cycles consisted of denaturing at 95C, annealing at 54C, and extension at 72C for 30 seconds each. Read out reactions were performed for 24 cycles and Step2 reactions were performed for 12 cycles.

Analysis of CRISPR screen readouts

An index for mapping NGS reads to TKOv3 sgRNA sequences was generated using Bowtie1. Fastq reads from NGS performed on the Illumina NextSeq platform were trimmed of adapter sequences and filtered for trimmed reads at least 17bp in length using Cutadapt. Trimmed reads were analyzed for read quality using FASTQC and mapped to TKOv3 using Bowtie1 without the SAM file output option and with options `-k 1 -v 1 -best`. Bowtie1 output was parsed using `sed`, `awk`, `cut`, `sort`, and `uniq` commands in Shell to generate counts files and make `cts` files that were processed using SLIDER. Hits with an $\text{FDR} < 10\%$ were nominated. The top 150 hits ranked by SLIDER score were analyzed using STRING. Pathway enrichment analysis was performed by supplying candidates with $\text{FDR} < 10\%$ to WebGestalt and Enrichr for enrichment of entries in WikiPathways.

SLIDER

The algorithm uses NGS readouts to determine the library-size normalized change in rank due to sorting (Δ) each sgRNA, statistically scores sgRNA for the significance of Δ using an asymmetric Laplace distribution with local and directional estimates of the diversity parameter (b). sgRNA p-values are combined using the weighted logit method and the Δ of each guide as its weight to arrive at a gene level sum that when appropriately scaled provides a SLIDER score that follows Student's t-distribution. The scaler is numerically by minimizing the L2E distance between the gene sums and a Student's t-distribution with two degrees of freedom. Genes are assigned p-values by looking up the SLIDER statistic in a Student's t-table with two degrees of freedom. Multiple comparisons are accounts for by computing a Benajmini-Hochberg estimate of the false discovery rate (FDR). For screens with multiple replicates, Stouffer's method is used to arrive at significance for each gene after accumulating evidence across replicates. The algorithm is implemented in R as a command line tool for scoring replicates with instructions on how to combine outputs from scoring multiple replicates to arrive at screen level summary statistics. The script and instructions are publicly available on GitHub at <https://github.com/LRPatel1/SLIDER> and described in further detail in Supplementary Data 1.

Precision recall analysis comparing SLIDER to drugZ and MAGeCK

NGS readcounts for sgRNA from the seven biological replicates scored by SLIDER were reanalyzed using DrugZ and MAGeCK. MAGeCK was run using the `-paired` option and `-log10(pos|score)` was used the gene's

score. For DrugZ, the NormZ score was used. Single gene perturbation experiments summarized in [Figure 3D](#) identified 15 true positives and 9 true negatives from 24 genes. Precision Recall analysis was performed using gene scores from each algorithm for these 24 genes and the R package `precec`. Confidence intervals were estimated by 25-fold subsampling performed by leaving none or one out.

Analysis of published screens

Read counts from screens by Gonatopoulos-Pournatzis et al., 2018; Simeonov et al., 2017; and Popa et al., 2019 were obtained from GEO deposits GSE112599, GSE98178, and GSE133692, respectively. Read counts from Timms et al., 2016 were downloaded from the published manuscript's supplementary files. Files in .cts format (see <https://github.com/LRPatel1/SLIDER>) were generated from downloaded counts files using `sed`, `awk`, and print commands in Unix. Screens by Simeonov et al. used tiling libraries instead of gene-targeting libraries. To generate .cts files for these screens, guides were sorted by genomic position, binned every 6 sgRNA, and labeled by the midpoint of genomic loci spanned by sgRNA in each bin instead of by a unique gene ID. For ROC analysis comparing results from SLIDER to published findings by Gonatopoulos-Pournatzis et al., 24 positive regulators nominated by sorting for high EGFP:mCherry cells carrying the Mef2d splicing reporter and 18 negative regulators nominated by sorting for low EGFP:mCherry cells were identified from [Figures 2](#) and [S2](#) of their manuscript for a total of 42 genes. SLIDER was used to analyze NGS readouts of screening replicates sorting for high EGFP:mCherry cells carrying the Mef2d splicing reporter. ROC was performed in R by the package `pROC` using SLIDER scores for these 42 genes, with the expectation that candidate positive regulators from the original study should be nominated by SLIDER analysis and candidate negative regulators should not be. Confidence intervals for area under the curve (AUC) were calculated by `pROC` using the Delong method.

Commercially obtained CRISPR knockout pools

CRISPR-Cas9 mediated knockout cell pools of ATF7IP, SETDB1, CNOT1, CNOT11, MAEA, WDR26, and YPEL5 in MCF10A cells were generated by Synthego Corporation (Redwood City, CA, USA). To generate these cells, Ribonucleoproteins containing the Cas9 protein and synthetic chemically modified sgRNA produced at Synthego were electroporated into the cells using Synthego's optimized protocol. Editing efficiency was assessed upon recovery 48 hours post electroporation and after expansion by extracting genomic DNA from a portion of the cells, PCR amplifying the targeted area, and analyzing chromatograms from Sanger sequencing using Synthego Inference of CRISPR Edits (ICE) software (ice.synthego.com). The editing efficiencies reported for each pool after expansion was 89%, 99%, 93%, 93%, 47%, 90%, and 84% for ATF7IP, SETDB1, CNOT1, CNOT11, MAEA, WDR26, and YPEL5, respectively. Edited pools were received on dry ice and stored in liquid nitrogen until the week of a single cell sorting appointment at the MD Anderson North Campus Flow Core, when cells were revived and expanded in 10cm plates with preparation of half of the cells for single cell sorting into 96-well plates and a frozen stock from the remainder. Clones expanded from 96-well plates were grown until 6-cm plates reached 70% confluence, when half of the cells were frozen as cryostocks and the other half was processed into DNA extracts and whole cell lysate for use in Western Blot and T7E1 assays. T7E1 assays were performed using the EnGen® Mutation Detection Kit per manufacturers protocol (NEB E3321S) and gene specific primers to amplify a ~500bp region containing PAM site targeted by Synthego to perform knockouts.

QUANTIFICATION AND STATISTICAL ANALYSIS

Statistical analysis performed by SLIDER is described above and in the description of SLIDER provided in supplementary materials. ROC, PRC, and statistical analyses presented to benchmark SLIDER's performance was performed using R. Copy number assays by ddPCR were analyzed using QuantaSoft, imported into Prism for visualization, and presented as copy number \pm Poisson error estimated from droplet variation. sgRNA counts of 6-guide containing pools determined by Sanger sequencing TOPO-clones of PCR products were compared before and after sorting using Chi-Squared test. Average values for GFP-A in bar charts from flow cytometry are presented as the mean \pm standard deviation and compared to non-targeting controls using Student's *t* test in Excel with $n = 4\sim 12$ independent cultures per condition. Raw flow cytometry data were analyzed using FlowJo. Heatmapped GFP-A intensities were compared using one-sided Z-tests with Bonferroni correction for multiple testing against LacZ controls with $n = 4\sim 12$ independent cultures per condition. With the exception of [Figure 5](#), protein abundances and qRT-PCR results presented in bar plots and charts are mean \pm standard deviation with $n = 3\sim 4$ biological replicates compared using Student's *t* test. Protein abundances in [Figure 5](#) are presented as mean \pm SEM and

statistical significance was determined by ANOVA followed by Student's t-tests for pairwise comparison to wild-type controls. Gene effect scores from DepMap were statistically compared to an expected non-essential score of 0 with left-tail z-tests, $n = 1070$ cell lines screened per gene assessed. The threshold for statistical significance in all tests was $\alpha < 0.05$. Symbols used to mark the level of significance in figure panels where comparisons were made along with their associated p values and the statistical-test used are specified in figure legends. Data was imported into Prism for visualization.